



## OPEN ACCESS

## EDITED BY

Wenjun Liu,  
Nanjing University of Information Science and  
Technology, China

## REVIEWED BY

Geeta Arora,  
Lovely Professional University, India  
Francisco Martínez,  
Polytechnic University of Cartagena, Spain

## \*CORRESPONDENCE

Appanah Rao Appadu  
✉ Rao.Appadu@mandela.ac.za

RECEIVED 19 July 2023

ACCEPTED 07 November 2023

PUBLISHED 18 December 2023

## CITATION

Appadu AR and Kelil AS (2023) Some finite  
difference methods for solving linear fractional  
KdV equation.  
*Front. Appl. Math. Stat.* 9:1261270.  
doi: 10.3389/fams.2023.1261270

## COPYRIGHT

© 2023 Appadu and Kelil. This is an  
open-access article distributed under the terms  
of the [Creative Commons Attribution License  
\(CC BY\)](https://creativecommons.org/licenses/by/4.0/). The use, distribution or reproduction  
in other forums is permitted, provided the  
original author(s) and the copyright owner(s)  
are credited and that the original publication in  
this journal is cited, in accordance with  
accepted academic practice. No use,  
distribution or reproduction is permitted which  
does not comply with these terms.

# Some finite difference methods for solving linear fractional KdV equation

Appanah Rao Appadu\* and Abey Sherif Kelil

Department of Mathematics and Applied Mathematics, Nelson Mandela University, University Way,  
Summerstrand, Gqeberha, South Africa

The time-fractional Korteweg de Vries equation can be viewed as a generalization of the classical KdV equation. The KdV equations can be applied in modeling tsunami propagation, coastal wave dynamics, and oceanic wave interactions. In this study, we construct two standard finite difference methods using finite difference methods with conformable and Caputo approximations to solve a time-fractional Korteweg-de Vries (KdV) equation. These two methods are named as FDMCA and FDMCO. FDMCA utilizes Caputo's derivative and a finite-forward difference approach for discretization, while FDMCO employs conformable discretization. To study the stability, we use the Von Neumann Stability Analysis for some fractional parameter values. We perform error analysis using  $L_1$  &  $L_\infty$  norms and relative errors, and we present results through graphical representations and tables. Our obtained results demonstrate strong agreement between numerical and exact solutions when the fractional operator is close to 1.0 for both methods. Generally, this study enhances our comprehension of the capabilities and constraints of FDMCO and FDMCA when used to solve such types of partial differential equations laying some ground for further research.

## KEYWORDS

fractional KdV equation, conformable and Caputo approximations, stability, finite difference methods, consistency, errors

## 1 Introduction

Fractional partial differential equations (FPDEs) are a generalization of classical partial differential equations (PDEs) that involve fractional derivatives of arbitrary order. The fractional derivatives in FPDEs account for non-local and non-linear phenomena, which are not captured by classical PDEs [1]. Physical models of real-world phenomenon often comprise considerable uncertainty due to a variety of variables. Due to their ability to model complex phenomena in physics and engineering, FPDEs have gained significant attention in recent years with their applications in signal processing, mechanics, plasma physics, finance, electricity, stochastic dynamical system, control theory, economics, and electrochemistry [2–4]. The numerical solution of fractional partial differential equations (FPDEs) has some challenges due to the non-local and non-linear nature of the fractional derivatives [5]. The Korteweg-de Vries (KdV) equation is a mathematical equation utilized to explain various physical phenomena related to non-linear wave evolution and interaction. It was developed based on the propagation of shallow water waves and is widely applied in areas such as fluid dynamics, aerodynamics, and continuum mechanics to model solitons, turbulence, and boundary layers, among others [6].

Several techniques have been developed to construct analytical and numerical methods for the KdV equation. These include the Adomian decomposition method [7], homotopy perturbation method [8], variational iteration method [9], finite difference method [10],

and finite volume method [11]. Aderogba and Appadu [12] recently used classical and multisymplectic schemes to solve some linearized KdV equations and dispersion analysis was studied. The authors in Appadu and Kelil [10] conducted a comparative study involving the application of the modified Adomain Decomposition Method and the classical finite difference method for solving some third-order and fifth-order KdV equations. Rostamy et al. [13] presented a numerical method for solving a class of fractional differential equations based on Bernstein polynomials basis; these matrices are utilized to reduce the multi-term orders fractional differential equation to a system of algebraic equations. Anwar et al. [14] studied the double Laplace formulae for the partial fractional integrals and derivatives in the sense of Caputo.

In studies, there are many formulations for the fractional differentiation and integration operators, including the Riemann-Liouville definition [15] and the Caputo definition [4]. A quite recent definition of the fractional derivative called the conformable fractional derivative, which can address the drawbacks of several definitions, was proposed by Khalil et al. [16]. The conformable operators generalize the classical idea of differentiability and allow for the generation of new and universal rates of variation. Therefore, the novelty of the study by Khalil et al. [16] was to check the validity of these operators together with classical finite difference approach in creating a new environment to look for more extended natural dispersive modeling scenarios. Toprakseven [17] derived a reliable finite difference method for fractional differential equations (FDEs) based on recently defined conformable fractional derivative. Li and Xu [18] constructed a time-space spectral method to investigate the solution of fractional partial differential equation. Lin and Xu [19] obtained the error estimate of the  $L_1$  scheme.

The plan of this study is detailed below. Section 2 describes the numerical experiment. In Section 3, we give some background on conformable fractional order derivative for the solution of non-homogeneous KdV equations. In Section 4, we propose a finite difference scheme known as the FDMCO scheme, which utilizes the conformable derivative. We have conducted a comprehensive study on stability analysis and consistency of the FDMCO scheme. Section 5 provides numerical results obtained from the FDMCO scheme, offering valuable insights into its performance, under various fractional parameter values  $\alpha \in (0, 1]$ . Section 6 proposes a finite difference scheme using Caputo fractional derivative and results shown in Section 7, respectively. Numerical profiles and relative errors for FDMCA scheme is given in subsection 7.2. Discussion of the comparison between the two schemes and conclusions are given in Section 8.

## 2 Numerical experiment

The Korteweg-de Vries (KdV) equation, introduced in 1895, describes weakly non-linear, dispersive waves, featuring non-linear advection and dispersion. The fractional Korteweg-de Vries (KdV) equation, as a generalization of the classical KdV equation, motivated by complex phenomena in dispersive media and takes the form:

$$\frac{\partial^\alpha u(t, x)}{\partial t^\alpha} + u \frac{\partial u(t, x)}{\partial x} + \frac{\partial^3 u(t, x)}{\partial x^3} = 0.$$

It uses fractional derivatives to analyze non-local effects and memory in wave propagation [4], providing insights into diverse problems by capturing intricate dynamics. These dynamics extend from fluid dynamics to plasma physics, encompassing long-range interactions, anomalous diffusion, and power-law behavior.

We consider the linear time-fractional non-homogeneous KdV equation [20] given by

$$\frac{\partial^\alpha u(t, x)}{\partial t^\alpha} + \frac{\partial u(t, x)}{\partial x} + \frac{\partial^3 u(t, x)}{\partial x^3} = 2t \cos(x), \quad (1)$$

where  $(t, x) \in [0, 1.0] \times [0, 3\pi]$ , and  $0 < \alpha \leq 1$ . The initial condition is

$$u(x, 0) = 0, \quad (2)$$

and the following boundary conditions are used:

$$u(0, t) = \frac{2t^{\alpha+1}}{\Gamma(2\alpha+1)}; \quad u(3\pi, t) = -\frac{2t^{\alpha+1}}{\Gamma(2\alpha+1)}. \quad (3)$$

The exact solution for this numerical experiment is given by Mohyud-Din et al. [20]

$$u(x, t) = 2 \cos(x) \frac{t^{\alpha+1}}{\Gamma(2\alpha+1)}.$$

We note that for  $\alpha = 1$ , the exact solution is  $u(x, t) = t^2 \cos(x)$ . In this study, we have used spatial step size  $\Delta x = \frac{\pi}{10}$ .

The relative error is calculated at a given spatial node  $x_j$  and time  $t_n$  using the following formula:

$$\text{Relative error} = \left| \frac{u(x_j, t_n) - U(x_j, t_n)}{u(x_j, t_n)} \right|, \quad (4)$$

subject to the condition that the exact solution  $u$  at the nodal point  $(x_j, t_n)$  is non-zero;  $U(x_j, t_n)$  represents the numerical solution at spatial domain  $x_j$  and time  $t_n$ . In this study, a scheme is considered efficient when its relative error is below 10%, and it is deemed satisfactory when the relative error falls within the range of 10% up to 25%. The scheme is considered to perform poorly if the relative error is greater than 25%. By relying on the given exact solution, the accuracy of the numerical solution and the performance (efficiency) of the scheme by computing  $L_1$  and  $L_\infty$  errors using the formulations:

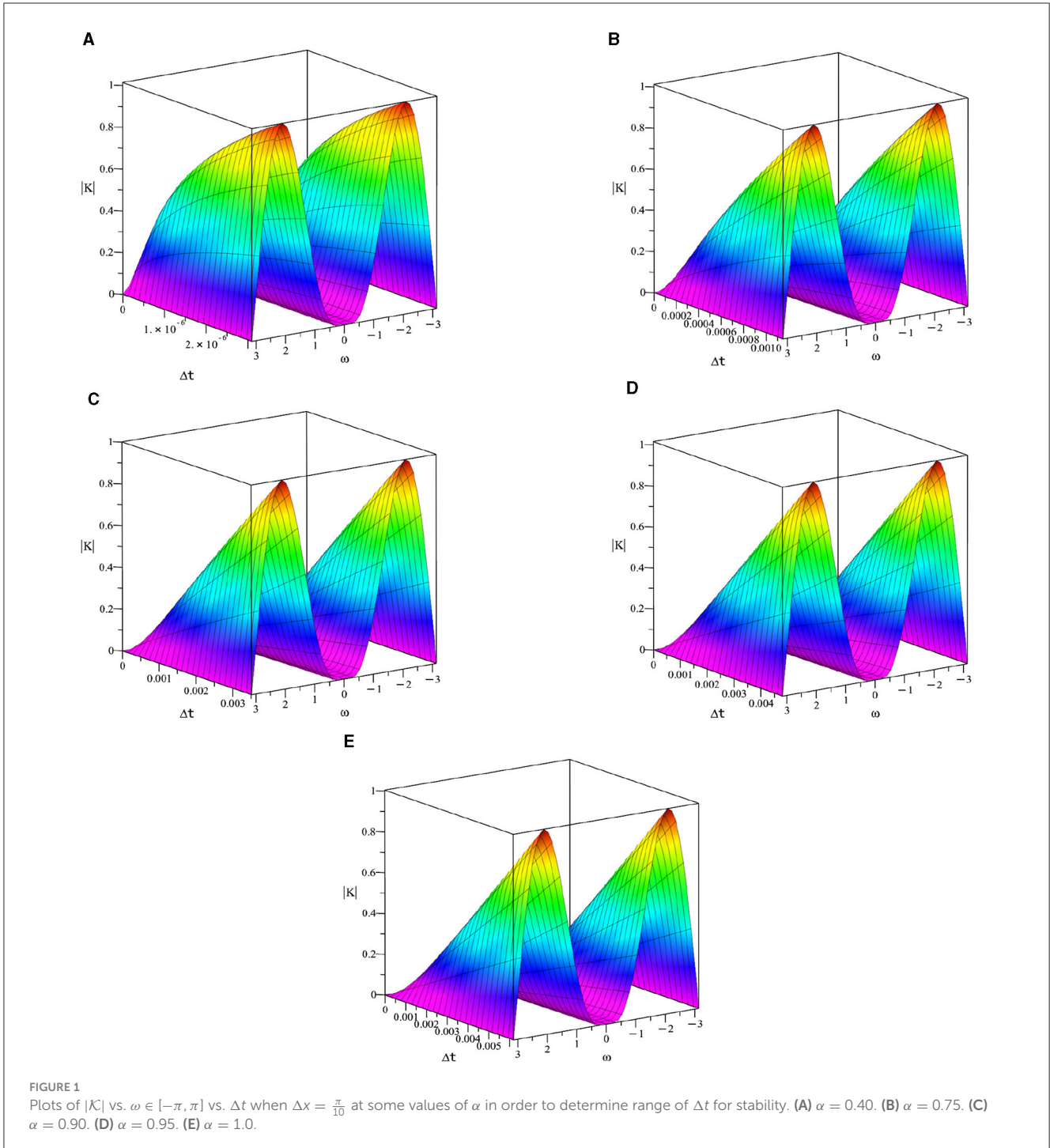
$$L_1 = \|U^{\text{exact}} - U_N\|_1 = h \sum_{j=0}^N |U_j^{\text{exact}} - (U_N)_j|; \quad \text{and}$$

$$L_\infty = \|U^{\text{exact}} - U_N\|_\infty = \max_j |U_j^{\text{exact}} - (U_N)_j|,$$

respectively.

## 3 Fractional derivatives

There are few definitions of fractional derivatives of order  $\alpha > 0$ . The most widely used are the Riemann-Liouville (RL), Caputo and conformable fractional derivatives [1, 16, 21–23].



**Definition 1.** The Riemann-Liouville fractional integral is defined by

$$J_t^\alpha f(t) = \frac{1}{\Gamma(\alpha)} \int_0^t (t-\tau)^{\alpha-1} f(\tau) d\tau, \quad \alpha > 0,$$

where

$$\Gamma(\alpha) = \int_0^{+\infty} x^{\alpha-1} e^{-x} dx,$$

is the Euler Gamma function [4].

**Definition 2.** The Caputo time-fractional derivative operator of order  $\alpha > 0$  ( $m-1 < \alpha \leq m$ ,  $m \in \mathbb{N}$ ) of a real valued function  $u(x, t)$  is defined as follows [24]:

$$\begin{aligned} \frac{\partial^\alpha u(x, t)}{\partial t^\alpha} &= J_t^{m-\alpha} \left[ \frac{\partial^m u(x, t)}{\partial t^m} \right], \\ &= \begin{cases} \frac{1}{\Gamma(m-\alpha)} \int_0^t (t-y)^{m-\alpha-1} \frac{\partial^m u(x, y)}{\partial y^m} dy, & m-1 < \alpha \leq m, \\ \frac{\partial^m u(x, t)}{\partial t^m}, & \alpha = m. \end{cases} \end{aligned} \tag{5}$$

TABLE 1 Range of values of  $\Delta t$  for stability of FDMCO scheme at some values of  $\alpha$ .

$\Delta x$	Values of the fractional parameter $\alpha$	Stability region for $\Delta t$
$\frac{\pi}{10}$	0.40	$(0, 3.10 \times 10^{-6})$
	0.75	$(0, 1.15 \times 10^{-3})$
	0.90	$(0, 3.51 \times 10^{-3})$
	0.95	$(0, 4.80 \times 10^{-3})$
	1.0	$(0, 6.20 \times 10^{-3})$

TABLE 2  $L_1$  and  $L_\infty$  errors using  $\Delta x = \frac{\pi}{10}$  when  $\alpha = 0.40$  at different values of time.

Time	value of $\Delta t$	$L_1$ error	$L_\infty$ error
0.01	$3 \times 10^{-6}$	$4.915480 \times 10^{-1}$	$9.870818 \times 10^{-2}$
	$2 \times 10^{-6}$	$4.458213 \times 10^{-1}$	$7.302036 \times 10^{-2}$
	$1 \times 10^{-6}$	$3.718674 \times 10^{-1}$	$7.341076 \times 10^{-2}$
	$5 \times 10^{-7}$	$3.918820 \times 10^{-1}$	$6.287411 \times 10^{-2}$
0.1	$3.0 \times 10^{-6}$	3.983312	$6.392576 \times 10^{-1}$
	$2.0 \times 10^{-6}$	4.003418	$6.413542 \times 10^{-1}$
	$1.0 \times 10^{-6}$	4.052244	$6.613390 \times 10^{-1}$
	$5.0 \times 10^{-7}$	3.996515	$7.001752 \times 10^{-1}$

Similarly, the Caputo space-fractional derivative operator  $\frac{\partial^\alpha u(x,t)}{\partial x^\alpha}$  of order  $\alpha > 0$  ( $m - 1 < \alpha \leq m$ ),  $m \in \mathbb{N}$  can be defined [22, 25]. It is worth noting that if  $u$  is sufficiently smooth [26], the fractional derivative  $\mathcal{D}_t^\alpha u$  recovers the typical first-order derivative  $u'(t)$  as  $\alpha \rightarrow 1^-$  [25].

Definition 3. [16]. For a function  $g: [0, \infty] \rightarrow \mathbb{R}$ , the conformable fractional derivative of  $g$  of order  $\alpha$  is defined by

$$D^\alpha \{g(z)\} = \lim_{\eta \rightarrow 0} \left( \frac{g(z + \eta z^{1-\alpha}) - g(z)}{\eta} \right). \tag{6}$$

Fundamental concepts and properties of conformable calculus are given in Khalil et al. [16] and Abdeljawad [21], and we note that the conformable derivative is chosen in order to preserve some of the classical properties of classical calculus [21]. Since other popular fractional derivatives (Caputo, RL) lack some of the natural properties of derivatives such as product rule, quotient rule, and chain rule, some authors such as Khalil et al. [16], and Abdelwajad [21] motivate the need to study conformable derivative to fill these gaps of preserving some natural properties of derivatives [4, 25].

Abdelwajad [21] approximated the time-fractional derivative using conformable approximation

$$\frac{\partial^\alpha u(x,t)}{\partial t^\alpha} = (\Delta t)^{1-\alpha} \frac{\partial u}{\partial t}. \tag{7}$$

if we let  $h = \eta t^{1-\alpha}$ , we thus have

$$\frac{\partial^\alpha g(t)}{\partial t^\alpha} = \lim_{\eta \rightarrow 0} \left( \frac{g(t + \eta t^{1-\alpha}) - g(t)}{\eta} \right)$$

TABLE 3  $L_1$  and  $L_\infty$  errors using  $\Delta x = \frac{\pi}{10}$  when  $\alpha = 0.75$  at different values of time.

Time	value of $\Delta t$	$L_1$ error	$L_\infty$ error
	$2 \times 10^{-3}$	$1.102763 \times 10^{-4}$	$2.181046 \times 10^{-5}$
	$1 \times 10^{-3}$	$4.379421 \times 10^{-4}$	$8.689720 \times 10^{-5}$
0.01	$5 \times 10^{-4}$	$9.717514 \times 10^{-4}$	$1.929225 \times 10^{-4}$
	$2.5 \times 10^{-4}$	$1.609101 \times 10^{-3}$	$3.191428 \times 10^{-4}$
	$1.25 \times 10^{-4}$	$2.363347 \times 10^{-3}$	$4.681859 \times 10^{-4}$
	$6.25 \times 10^{-5}$	$3.251182 \times 10^{-3}$	$6.576396 \times 10^{-4}$
0.1	$2 \times 10^{-3}$	$9.379574 \times 10^{-2}$	$2.390875 \times 10^{-2}$
	$1.0 \times 10^{-3}$	$1.321475 \times 10^{-1}$	$3.366855 \times 10^{-2}$
	$5.0 \times 10^{-4}$	$1.755505 \times 10^{-1}$	$4.484513 \times 10^{-2}$
1.0	$2.0 \times 10^{-3}$	12.272151	3.358171
	$1.0 \times 10^{-3}$	15.182849	4.234356
	$5.0 \times 10^{-4}$	18.233762	5.248255
	$2.5 \times 10^{-4}$	21.417630	6.427455

TABLE 4  $L_1$  and  $L_\infty$  errors using  $\Delta x = \frac{\pi}{10}$  when  $\alpha = 0.90$  at different values of time.

Time	value of $\Delta t$	$L_1$ error	$L_\infty$ error
0.01	$2 \times 10^{-3}$	$5.220832 \times 10^{-5}$	$1.035473 \times 10^{-5}$
	$1 \times 10^{-3}$	$5.274179 \times 10^{-5}$	$1.045404 \times 10^{-5}$
	$5 \times 10^{-4}$	$1.248522 \times 10^{-4}$	$2.477435 \times 10^{-5}$
0.1	$4 \times 10^{-3}$	$1.156128 \times 10^{-2}$	$2.454653 \times 10^{-3}$
	$2 \times 10^{-3}$	$1.772734 \times 10^{-2}$	$3.860118 \times 10^{-3}$
	$1 \times 10^{-3}$	$2.416105 \times 10^{-2}$	$5.352817 \times 10^{-3}$
	$5 \times 10^{-4}$	$3.099005 \times 10^{-2}$	$6.960574 \times 10^{-3}$
1.0	$4.0 \times 10^{-3}$	2.260338	$6.379577 \times 10^{-1}$
	$2.0 \times 10^{-3}$	2.759944	$7.777959 \times 10^{-1}$
	$1 \times 10^{-3}$	3.296322	$9.237007 \times 10^{-1}$
	$5 \times 10^{-4}$	3.877546	1.075498

$$\begin{aligned}
 &= t^{1-\alpha} \lim_{h \rightarrow 0} \left( \frac{g(t+h) - g(t)}{h} \right) \\
 &= t^{1-\alpha} \frac{\partial g(t)}{\partial t}.
 \end{aligned} \tag{8}$$

Hence, we can approximate  $\frac{\partial^\alpha u(x,t)}{\partial t^\alpha}$  by  $(\Delta t)^{1-\alpha} \left[ \frac{U_j^{n+1} - U_j^{n-1}}{2 \cdot (\Delta t)} \right]$ , if we choose to use a central difference approximation for  $\frac{\partial u}{\partial t}$ .

For some properties of conformable fractional derivatives, we refer the reader to Khalil et al. [16], Abdelwajad [21], Atangana et al. [28], and Atangana and Secer [29].

Yokus et al. [27] conducted a comparative study on the time fractional Burgers-Fisher equation, specifically focusing on the Caputo and conformable approximations; and the authors utilized the sub-equation method as an analytical approach for

TABLE 5  $L_1$  and  $L_\infty$  errors using  $\Delta x = \frac{\pi}{10}$  when  $\alpha = 0.95$  at different values of time.

Time	value of time step $\Delta t$	$L_1$ error	$L_\infty$ error
0.01	$2 \times 10^{-3}$	$3.429144 \times 10^{-5}$	$6.802174 \times 10^{-6}$
	$1 \times 10^{-3}$	$1.748902 \times 10^{-5}$	$3.467188 \times 10^{-6}$
	$5 \times 10^{-4}$	$4.257475 \times 10^{-5}$	$8.448452 \times 10^{-6}$
	$6.25 \times 10^{-5}$	$1.233221 \times 10^{-4}$	$2.447138 \times 10^{-5}$
	$3.125 \times 10^{-5}$	$1.521587 \times 10^{-4}$	$3.019341 \times 10^{-5}$
0.1	$4 \times 10^{-3}$	$4.418312 \times 10^{-3}$	$8.813985 \times 10^{-4}$
	$2 \times 10^{-3}$	$6.810338 \times 10^{-3}$	$1.403634 \times 10^{-3}$
	$1 \times 10^{-3}$	$9.188834 \times 10^{-3}$	$1.921917 \times 10^{-3}$
	$5 \times 10^{-4}$	$1.164239 \times 10^{-2}$	$2.463030 \times 10^{-3}$
	$6.25 \times 10^{-5}$	$1.947890 \times 10^{-2}$	$4.225262 \times 10^{-3}$
	$3.125 \times 10^{-5}$	$2.225729 \times 10^{-2}$	$4.860104 \times 10^{-3}$
1.0	$4.0 \times 10^{-3}$	$9.429881 \times 10^{-1}$	$2.630962 \times 10^{-1}$
	$2.0 \times 10^{-3}$	1.136734	$3.190145 \times 10^{-1}$
	$1 \times 10^{-3}$	1.336796	$3.766654 \times 10^{-1}$
	$5 \times 10^{-4}$	1.543195	$4.358764 \times 10^{-1}$

TABLE 6  $L_1$  and  $L_\infty$  errors using  $\Delta x = \frac{\pi}{10}$  when  $\alpha = 1.0$  at different values of time.

Time	value of $\Delta t$	$L_1$ error	$L_\infty$ error
0.01	$2 \times 10^{-3}$	$2.016202 \times 10^{-5}$	$4.000000 \times 10^{-6}$
	$1 \times 10^{-3}$	$1.871088 \times 10^{-7}$	$1.492947 \times 10^{-7}$
	$5 \times 10^{-4}$	$5.672332 \times 10^{-8}$	$3.893163 \times 10^{-8}$
	$2.5 \times 10^{-4}$	$2.429446 \times 10^{-8}$	$1.138296 \times 10^{-8}$
	$1.25 \times 10^{-4}$	$1.618922 \times 10^{-8}$	$4.498410 \times 10^{-9}$
	$6.25 \times 10^{-5}$	$1.552439 \times 10^{-8}$	$2.777437 \times 10^{-9}$
	$3.125 \times 10^{-5}$	$1.548392 \times 10^{-8}$	$2.691299 \times 10^{-9}$
	$2 \times 10^{-3}$	$1.604704 \times 10^{-5}$	$4.171814 \times 10^{-6}$
0.1	$1 \times 10^{-3}$	$1.551552 \times 10^{-5}$	$3.130329 \times 10^{-6}$
	$5 \times 10^{-4}$	$1.538230 \times 10^{-5}$	$2.868913 \times 10^{-6}$
	$2.5 \times 10^{-4}$	$1.535570 \times 10^{-5}$	$2.803494 \times 10^{-6}$
	$1.25 \times 10^{-4}$	$1.535207 \times 10^{-5}$	$2.787135 \times 10^{-6}$
	$6.25 \times 10^{-5}$	$1.535225 \times 10^{-5}$	$2.785928 \times 10^{-6}$
	$3.125 \times 10^{-5}$	$1.535232 \times 10^{-5}$	$2.785985 \times 10^{-6}$
1.0	$2.0 \times 10^{-3}$	$1.515394 \times 10^{-2}$	$3.112947 \times 10^{-3}$
	$1.0 \times 10^{-3}$	$1.515305 \times 10^{-2}$	$3.113227 \times 10^{-3}$
	$5.0 \times 10^{-4}$	$1.515283 \times 10^{-2}$	$3.113287 \times 10^{-3}$
	$2.5 \times 10^{-4}$	$1.515277 \times 10^{-2}$	$3.113301 \times 10^{-3}$
	$1.25 \times 10^{-4}$	$1.515276 \times 10^{-2}$	$3.113305 \times 10^{-3}$
	$6.25 \times 10^{-5}$	$1.515276 \times 10^{-2}$	$3.113306 \times 10^{-3}$
	$3.125 \times 10^{-5}$	$1.515275 \times 10^{-2}$	$3.113306 \times 10^{-3}$

their investigation. Yokus et al. [30] examined various methods, including analytical, numerical, and approximate analytical techniques, to solve the time-fractional non-linear Burger-Fisher equation. Specifically, they employed the  $(1/G)'$ -expansion method, the finite difference method (FDM), and the Laplace perturbation method (LPM). Pedram et al. [31] studied the effect of white noise on conformable time and space fractional KdV and BBM equations by transforming these equations with external noise into homogeneous conformable time and space fractional KdV and BBM equations and solved these equations using the modified Kudryashov method. In Arafa et al. [32], the authors employed a time-fractional conformable derivative to investigate an unsteady convection-radiation interaction flow of power-law non-Newtonian nanofluids. Mous et al. [33] investigated the numerical solution of a coupled system of two-dimensional (2D) Burgers' equations with fractional conformable time derivatives, and they tried to capture the interaction between non-linear convection processes and diffusive viscous processes. Azerad and Bourharguane [34] constructed some finite difference schemes to solve a fractional diffusion/anti-diffusion equation, and they also studied the stability, consistency, and convergence of these schemes.

## 4 Finite difference method using conformable approximation

### 4.1 Derivation

We consider Equation (1) and discretise  $\frac{\partial u}{\partial x}$  and  $\frac{\partial^3 u}{\partial x^3}$  using central difference approximations and approximate  $\frac{\partial^\alpha u(x,t)}{\partial t^\alpha}$  using (??). This gives the following scheme which we term as "finite difference method using conformable derivative" abbreviated as FDMCO:

$$(\Delta t)^{1-\alpha} \left( \frac{U_j^{n+1} - U_j^{n-1}}{2(\Delta t)} \right) + \left( \frac{U_{j+1}^n - U_{j-1}^n}{2(\Delta x)} \right) + \left( \frac{U_{j+2}^n - 2U_{j+1}^n + 2U_{j-1}^n - U_{j-2}^n}{2(\Delta x)^3} \right) = 2t_n \cos(x_j). \tag{9}$$

Equation (9) is rewritten as

$$U_j^{n+1} = U_j^{n-1} - \frac{(\Delta t)^\alpha}{\Delta x} (U_{j+1}^n - U_{j-1}^n) - \frac{(\Delta t)^\alpha}{(\Delta x)^3} (U_{j+2}^n - 2U_{j+1}^n + 2U_{j-1}^n - U_{j-2}^n) + 4(\Delta t)^\alpha t_n \cos(x_j), \tag{10}$$

We need to use another scheme to obtain solution at second time level. The scheme is given by

$$(\Delta t)^{1-\alpha} \left( \frac{U_j^2 - U_j^1}{\Delta t} \right) + \left( \frac{U_{j+1}^1 - U_{j-1}^1}{2(\Delta x)} \right) + \left( \frac{U_{j+2}^1 - 2U_{j+1}^1 + 2U_{j-1}^1 - U_{j-2}^1}{2(\Delta x)^3} \right) = 2t_1 \cos(x_j). \tag{11}$$

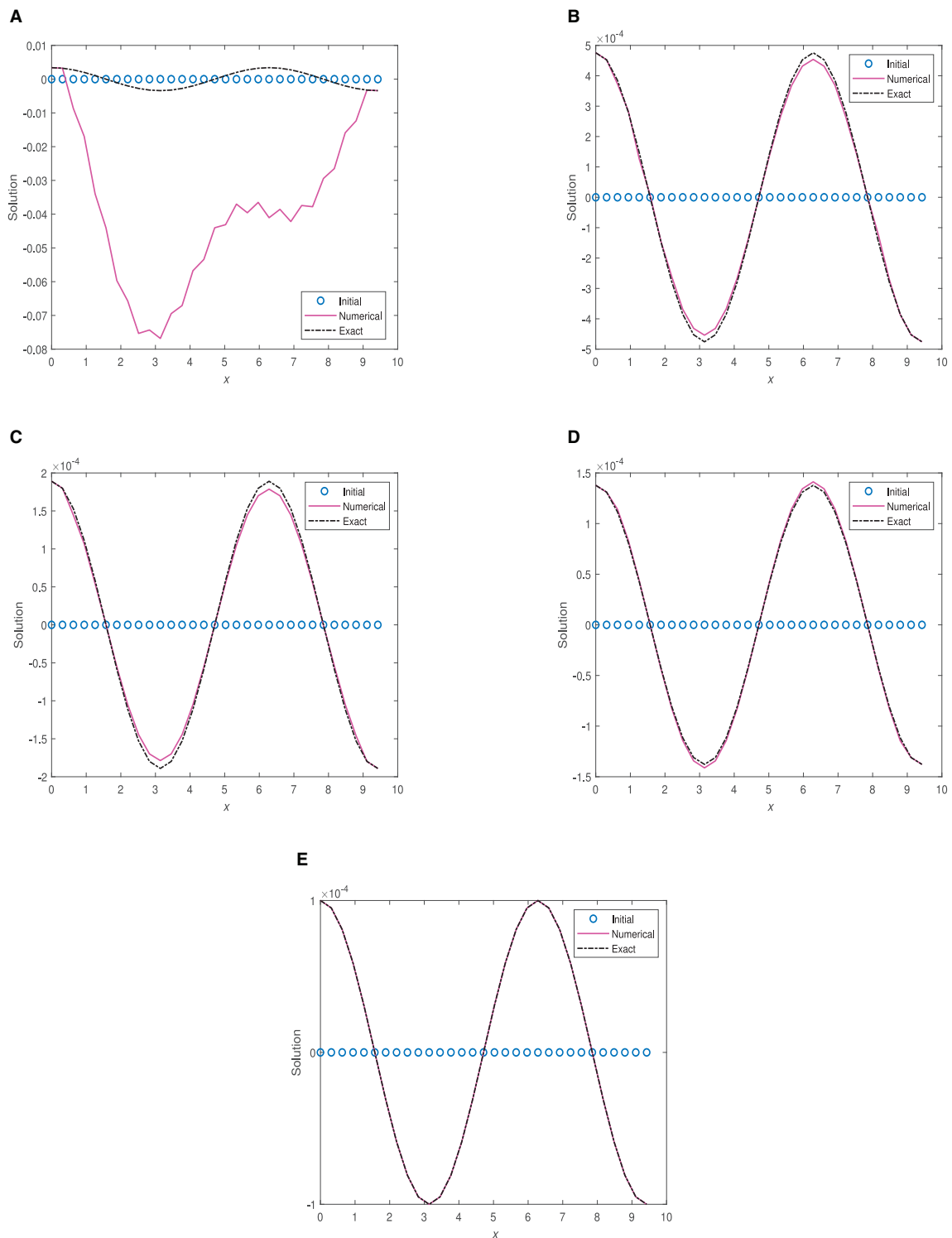


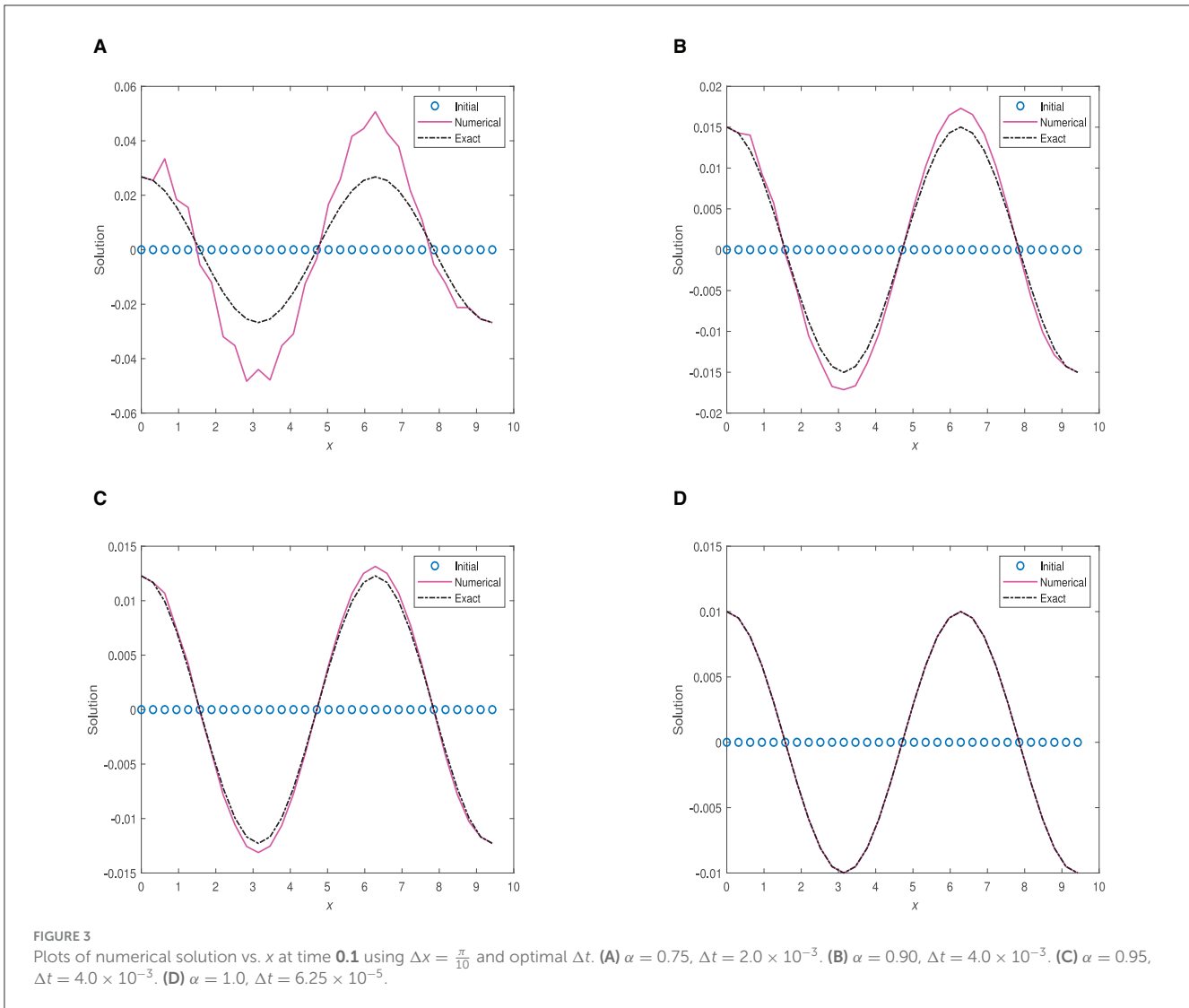
**FIGURE 2**  
 Plots of numerical solution vs.  $x$  at time  $0.01$  using  $\Delta x = \frac{\pi}{10}$  and optimal  $\Delta t$ . **(A)**  $\alpha = 0.40$ ,  $\Delta t = 1.0 \times 10^{-6}$ . **(B)**  $\alpha = 0.75$ ,  $\Delta t = 2.0 \times 10^{-3}$ . **(C)**  $\alpha = 0.90$ ,  $\Delta t = 2.0 \times 10^{-3}$ . **(D)**  $\alpha = 0.95$ ,  $\Delta t = 1.0 \times 10^{-3}$ . **(E)**  $\alpha = 1.0$ ,  $\Delta t = 3.125 \times 10^{-5}$ .

which can be rewritten as

$$-\frac{(\Delta t)^\alpha}{2(\Delta x)^3} (U_{j+2}^1 - 2U_{j+1}^1 + 2U_{j-1}^1 - U_{j-2}^1), \tag{12}$$

$$U_j^2 = U_j^1 - \frac{(\Delta t)^\alpha}{2(\Delta x)} (U_{j+1}^1 - U_{j-1}^1)$$

where  $U_j^1$  is the initial solution at the grid point  $x_j$ .



### 4.2 Stability analysis

To obtain the stability region of the scheme, we make use of Von Neumann Stability Analysis. We consider Equation (10) with source term being 0, i.e.,

$$U_j^{n+1} = U_j^{n-1} - \frac{(\Delta t)^\alpha}{\Delta x} (U_{j+1}^n - U_{j-1}^n) - \frac{(\Delta t)^\alpha}{(\Delta x)^3} (U_{j+2}^n - 2U_{j+1}^n + 2U_{j-1}^n - U_{j-2}^n). \quad (13)$$

We use the ansatz  $U_j^n = \xi^n e^{I\theta jh}$  where  $\xi$  is the amplification factor,  $\theta$  is the wave number and  $I = \sqrt{-1}$ . This gives

$$\xi = \xi^{-1} - \frac{(\Delta t)^\alpha}{\Delta x} (e^{I\omega} - e^{-I\omega}) - \frac{(\Delta t)^\alpha}{(\Delta x)^3} (e^{2I\omega} - 2e^{I\omega} + 2e^{-I\omega} - e^{-2I\omega}), \quad (14)$$

where  $\omega = \theta h$ . Equation (14) can be rewritten as

$$\xi^2 = 1 - \frac{(\Delta t)^\alpha}{\Delta x} \xi (2I \sin(\omega))$$

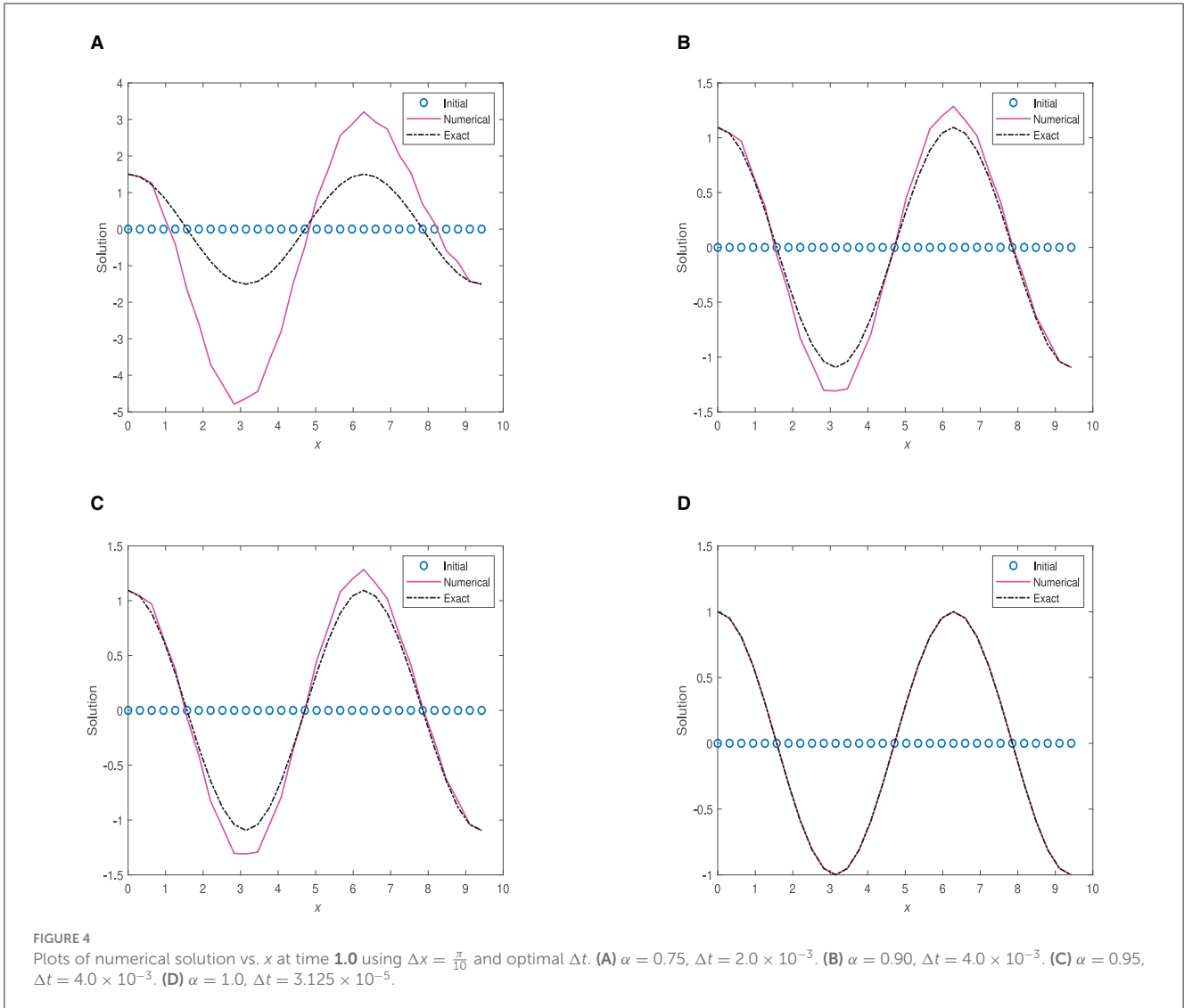
$$- \frac{(\Delta t)^\alpha}{(\Delta x)^3} (2I \sin(2\omega) - 4I \sin(\omega)) \xi. \quad (15)$$

The quadratic equation in Equation (15) can be rewritten as  $\xi^2 + IK\xi - 1 = 0$ , where

$$K = \frac{(\Delta t)^\alpha}{\Delta x} (2 \sin(\omega)) + \frac{(\Delta t)^\alpha}{(\Delta x)^3} (2 \sin(2\omega) - 4 \sin(\omega)). \quad (16)$$

Solving Equation (15) gives  $\xi_1 = \frac{-IK + \sqrt{4 - K^2}}{2}$  and  $\xi_2 = \frac{-IK - \sqrt{4 - K^2}}{2}$ , where  $\xi_1$  and  $\xi_2$  are amplification factors of physical and computational nodes, respectively. To obtain the region of stability, we must have  $4 - K^2 > 0$ ; i.e.,  $|K| < 2$ , this then gives  $|\xi_1| = 1$  and  $|\xi_2| = 1$ . We solve

$$|K| = \left| 2 \frac{(\Delta t)^\alpha}{\Delta x} \sin(\omega) + \frac{(\Delta t)^\alpha}{(\Delta x)^3} (2 \sin(2\omega) - 4 \sin(\omega)) \right| < 2. \quad (17)$$



Plots of  $|K|$  vs.  $\omega \in [-\pi, \pi]$  vs.  $\Delta t$  are displayed in Figure 1 in order to obtain range of values of  $\Delta t$  for which  $|K| < 2$ . We fix  $\Delta x = \frac{\pi}{10}$  and consider five values of  $\alpha$ : 0.40, 0.75, 0.90, 0.95, and 1.0. We obtain range of values of  $\Delta t$  for stability for the five cases in Table 1.

We can see from Table 1 that the stability region becomes more restricted as  $\alpha$  is decreased from 1.0.

### 4.3 Consistency

We apply Taylor series expansion about  $(t_n, x_j)$  to the discretized scheme in Equation (10) to obtain

$$\begin{aligned}
 & U + (\Delta t)U_t + \frac{(\Delta t)^2}{2}U_{tt} + \frac{(\Delta t)^3}{6}U_{ttt} + \mathcal{O}((\Delta t)^4) \\
 &= U - (\Delta t)U_t + \frac{(\Delta t)^2}{2}U_{tt} - \frac{(\Delta t)^3}{6}U_{ttt} + \mathcal{O}((\Delta t)^4) \\
 &- \frac{(\Delta t)^\alpha}{\Delta x} \left[ U + (\Delta x)U_x + \frac{(\Delta x)^2}{2!}U_{xx} + \frac{(\Delta x)^3}{3!}U_{xxx} \right.
 \end{aligned}$$

$$\begin{aligned}
 & \left. - \left( U - (\Delta x)U_x + \frac{(\Delta x)^2}{2!}U_{xx} - \frac{(\Delta x)^3}{3!}U_{xxx} \right) + \dots \right] \\
 &- \frac{(\Delta t)^\alpha}{(\Delta x)^3} \left[ \left( U + 2(\Delta x)U_x + \frac{(2\Delta x)^2}{2}U_{xx} + \frac{(2\Delta x)^3}{3!}U_{xxx} \right. \right. \\
 &+ \frac{(2\Delta x)^4}{4!}U_{xxxx} + \mathcal{O}((\Delta x)^5) \left. \right) - 2 \left( U + (\Delta x)U_x + \frac{(\Delta x)^2}{2!}U_{xx} \right. \\
 &+ \frac{(\Delta x)^3}{3!}U_{xxx} + \frac{(\Delta x)^4}{4!}U_{xxxx} + \mathcal{O}((\Delta x)^5) \left. \right) \\
 &+ 2 \left( U - (\Delta x)U_x + \frac{(\Delta x)^2}{2!}U_{xx} - \frac{(\Delta x)^3}{3!}U_{xxx} + \right. \\
 &\left. \frac{(\Delta x)^4}{4!}U_{xxxx} + \mathcal{O}((\Delta x)^5) \right) - \left( U - 2(\Delta x)U_x + \frac{(2(\Delta x))^2}{2!}U_{xx} \right. \\
 &\left. - \frac{(2(\Delta x))^3}{3!}U_{xxx} + \frac{(2(\Delta x))^4}{4!}U_{xxxx} + \mathcal{O}((\Delta x)^5) \right) \left. \right] \\
 &+ 4 \cdot (\Delta t)^\alpha \cdot t_n \cos(x_j),
 \end{aligned}$$

which gives

$$\begin{aligned}
 & \frac{\partial U}{\partial t} + \frac{(\Delta t)^\alpha}{\Delta t}U_x + \frac{(\Delta t)^\alpha}{\Delta t}U_{xxx} - 2 \frac{(\Delta t)^\alpha}{\Delta t}t_n \cos(x_j) \\
 &= -\frac{1}{3!}(\Delta t)^2U_{ttt} - \frac{1}{3!}(\Delta x)^2 \frac{(\Delta t)^\alpha}{\Delta t}U_{xxx} + \mathcal{O}((\Delta x)^2). \quad (18)
 \end{aligned}$$



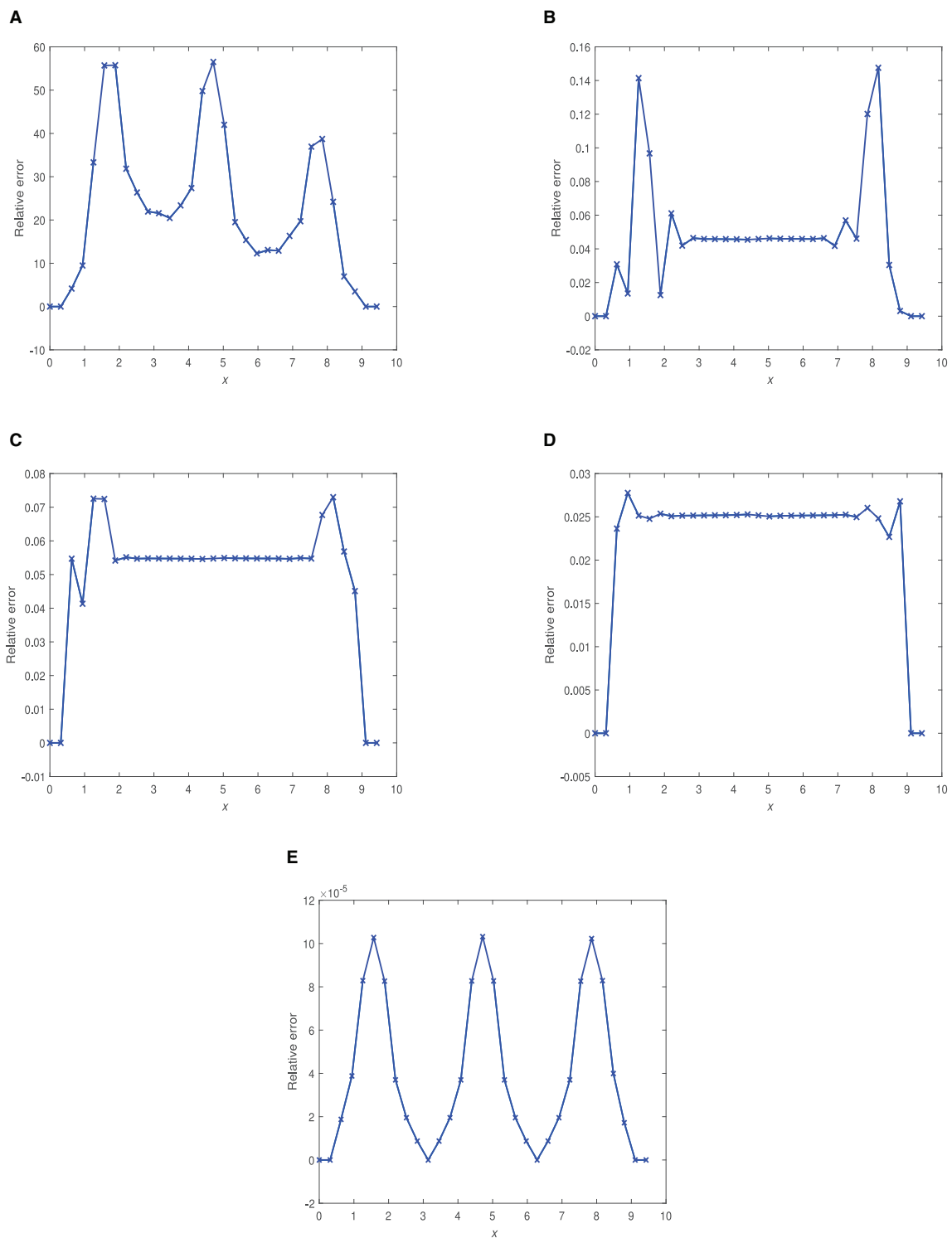


**FIGURE 5** Plots of relative errors vs.  $x$  at time **0.01** using  $\Delta x = \frac{\pi}{10}$  and optimal  $\Delta t$ . **(A)**  $\alpha = 0.40$ ,  $\Delta t = 1.0 \times 10^{-6}$ . **(B)**  $\alpha = 0.75$ ,  $\Delta t = 2.0 \times 10^{-3}$ . **(C)**  $\alpha = 0.90$ ,  $\Delta t = 2.0 \times 10^{-3}$ . **(D)**  $\alpha = 0.95$ ,  $\Delta t = 1.0 \times 10^{-3}$ . **(E)**  $\alpha = 1.0$ ,  $\Delta t = 3.125 \times 10^{-5}$ .

If we multiply both sides of Equation (18) by  $(\Delta t)^{1-\alpha}$ , we obtain

$$\frac{\partial^\alpha U}{\partial t^\alpha} + \frac{\partial U}{\partial x} + \frac{\partial^3 U}{\partial t^3} - 2t_n \cos(x_j)$$

$$= -\frac{(\Delta t)^{3-\alpha}}{3!} U_{ttt} - \frac{(\Delta x)^2}{3!} U_{xxx} + \mathcal{O}((\Delta x)^2 (\Delta t)^{1-\alpha}). \quad (19)$$

Thus, the FDMCO scheme is consistent with the PDE in Equation (1) and is accurate of order  $(3 - \alpha)$  in time and accurate of order 2 in space.

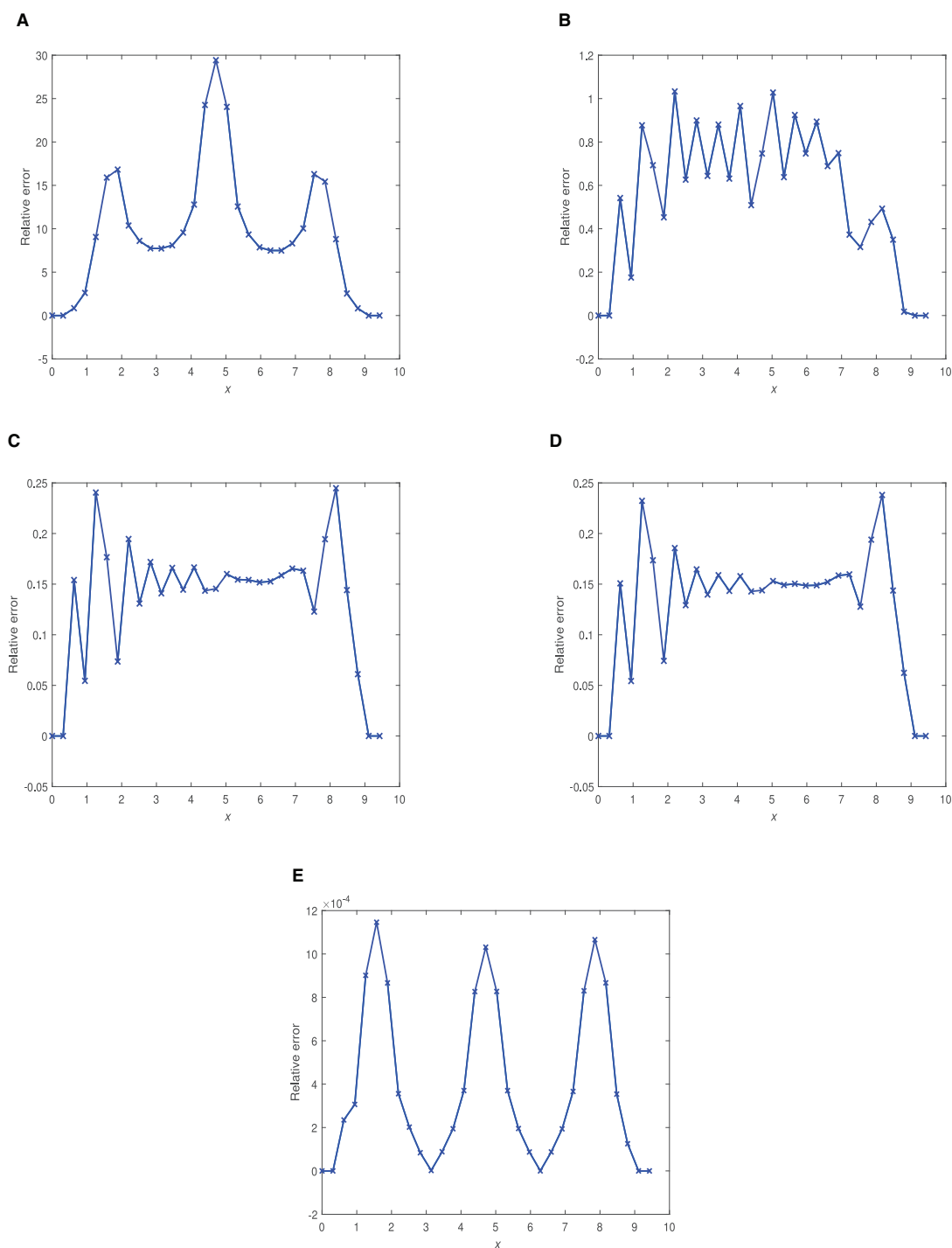


**FIGURE 6** Plots of relative errors vs.  $x$  at time  $0.1$  using  $\Delta x = \frac{\pi}{10}$  and optimal  $\Delta t$ . **(A)**  $\alpha = 0.40$ ,  $\Delta t = 1.0 \times 10^{-6}$ . **(B)**  $\alpha = 0.75$ ,  $\Delta t = 2.0 \times 10^{-3}$ . **(C)**  $\alpha = 0.90$ ,  $\Delta t = 4.0 \times 10^{-3}$ . **(D)**  $\alpha = 0.95$ ,  $\Delta t = 1.0 \times 10^{-3}$ . **(E)**  $\alpha = 1.0$ ,  $\Delta t = 3.125 \times 10^{-5}$ .

## 5 Numerical results from FDMCO

### 5.1 Display of $L_1$ and $L_\infty$ errors

We present in [Tables 2–6](#), the  $L_1$  and  $L_\infty$  errors at the three different times and some different values of  $\Delta t$  for the five cases:

$\alpha = 0.40, 0.75, 0.90, 0.95,$  and  $1.0$ . We note that in all numerical experiments, we chose  $\Delta x = \frac{\pi}{10}$ . The values of  $\Delta t$  are chosen from the range of values of  $\Delta t$  for which the scheme is stable as explained in [Table 1](#).

We can see from [Tables 5, 6](#) that FDMCO scheme performs well for the considered experiment for  $\alpha = 0.95, 1.0$ , respectively, at

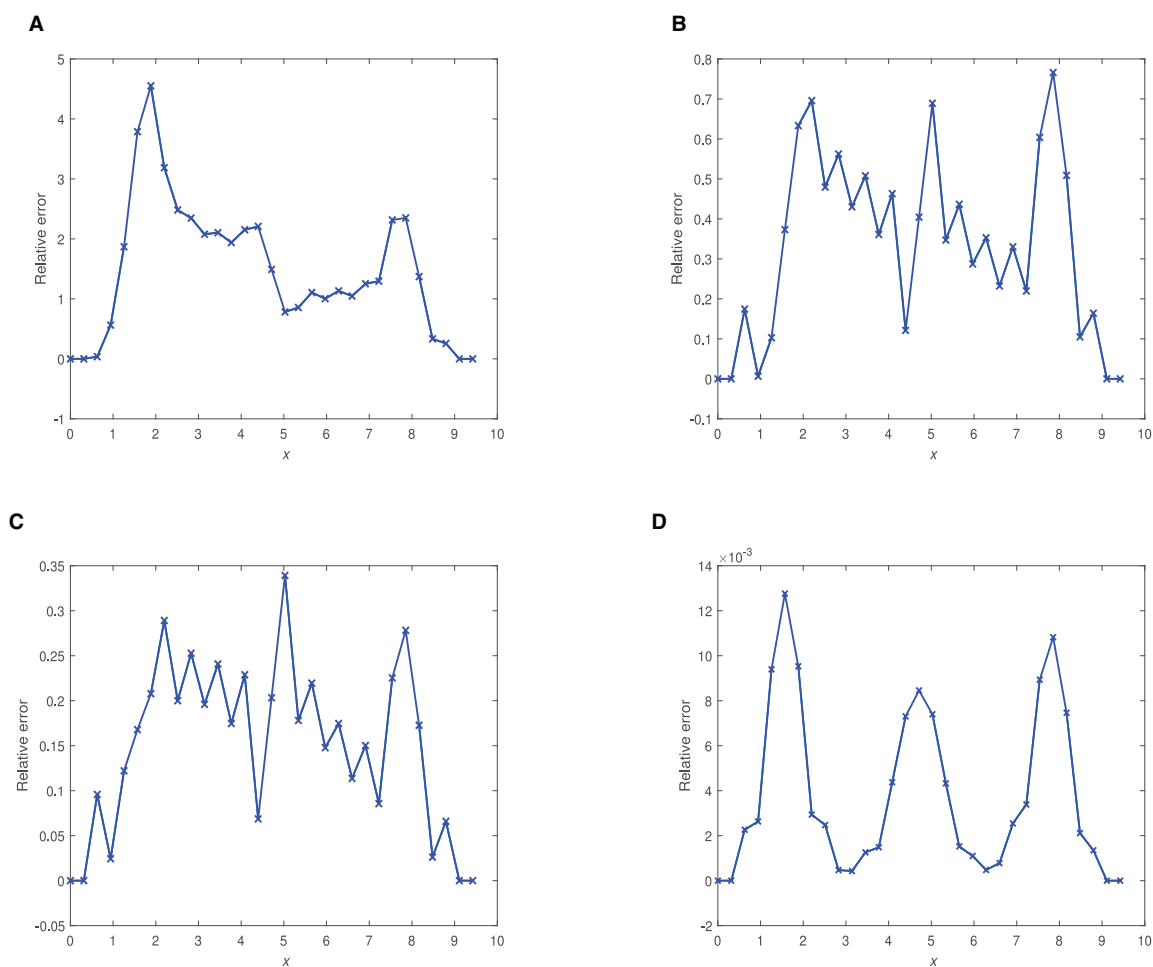


FIGURE 7  
 Plots of relative errors vs.  $x$  at time  $1.0$  using  $\Delta x = \frac{\pi}{10}$  and optimal  $\Delta t$ . (A)  $\alpha = 0.75$ ,  $\Delta t = 2.0 \times 10^{-3}$ . (B)  $\alpha = 0.90$ ,  $\Delta t = 4.0 \times 10^{-3}$ . (C)  $\alpha = 0.95$ ,  $\Delta t = 4.0 \times 10^{-3}$ . (D)  $\alpha = 1.0$ ,  $\Delta t = 3.125 \times 10^{-5}$ .

time 0.01, 0.1. The FDMCO scheme performs quite well at time 1.0 only for the case when  $\alpha = 1.0$ .

### 5.2 Numerical profiles and relative errors: FDMCO

We plot numerical solutions vs.  $x$  for five  $\alpha$  values at times 0.01, 0.1, and 1.0 using the optimal  $\Delta t$ .

Figure 2 illustrates 2D plots of the numerical solution vs.  $x$  at time 0.01. Figure 3 presents graphs of the numerical solution with respect to  $x$  at time 0.1.

Figure 4 demonstrates plots of the numerical solution vs.  $x$  at time 1.0. The computations utilized  $\Delta x = \frac{\pi}{10}$  and the optimal  $\Delta t$  for fractional parameters  $\alpha = 0.40, 0.75, 0.90, 0.95, 1.0$ .

Additionally, Figures 5–7 display graphs of the relative errors with respect to  $x$  at the three different time values.

Figure 5 depicts graphs for the relative errors vs.  $x$  at time 0.01 using the FDMCO scheme with  $\Delta x = \frac{\pi}{10}$  and optimal  $\Delta t$  for five different fractional parameters  $\alpha = 0.40, 0.75, 0.90, 0.95, 1.0$ . We have plotted the relative error by ignoring three nodal points ( $x = \frac{\pi}{2} = 1.571, \frac{3\pi}{2} = 4.712, \frac{5\pi}{2} = 7.854$ ) as the exact solution at these points lies in the range  $10^{-22}$  to  $10^{-4}$  (very close to zero) for the five different values of the fractional parameter  $\alpha$ .

Corresponding plots of relative errors vs.  $x$  at time 0.1 and 1.0 are shown in Figures 6, 7.

### 5.3 Discussion of results: FDMCO

At  $\alpha = 0.40$  and time 0.01, the scheme exhibits poor performance, with the  $L_1$  error of order  $10^{-1}$ . As time increases to 0.1, the scheme’s performance worsens, and the  $L_\infty$  error follows a similar trend, ranging from approximately  $10^{-2}$  to  $10^{-1}$ .

At  $\alpha = 0.75$  and time 0.01, the scheme performs quite well, with the  $L_1$  error at  $10^{-4}$  and the  $L_\infty$  error ranging from  $10^{-5}$  to  $10^{-4}$ . However, when the time is increased to 0.1, the  $L_1$  errors increase

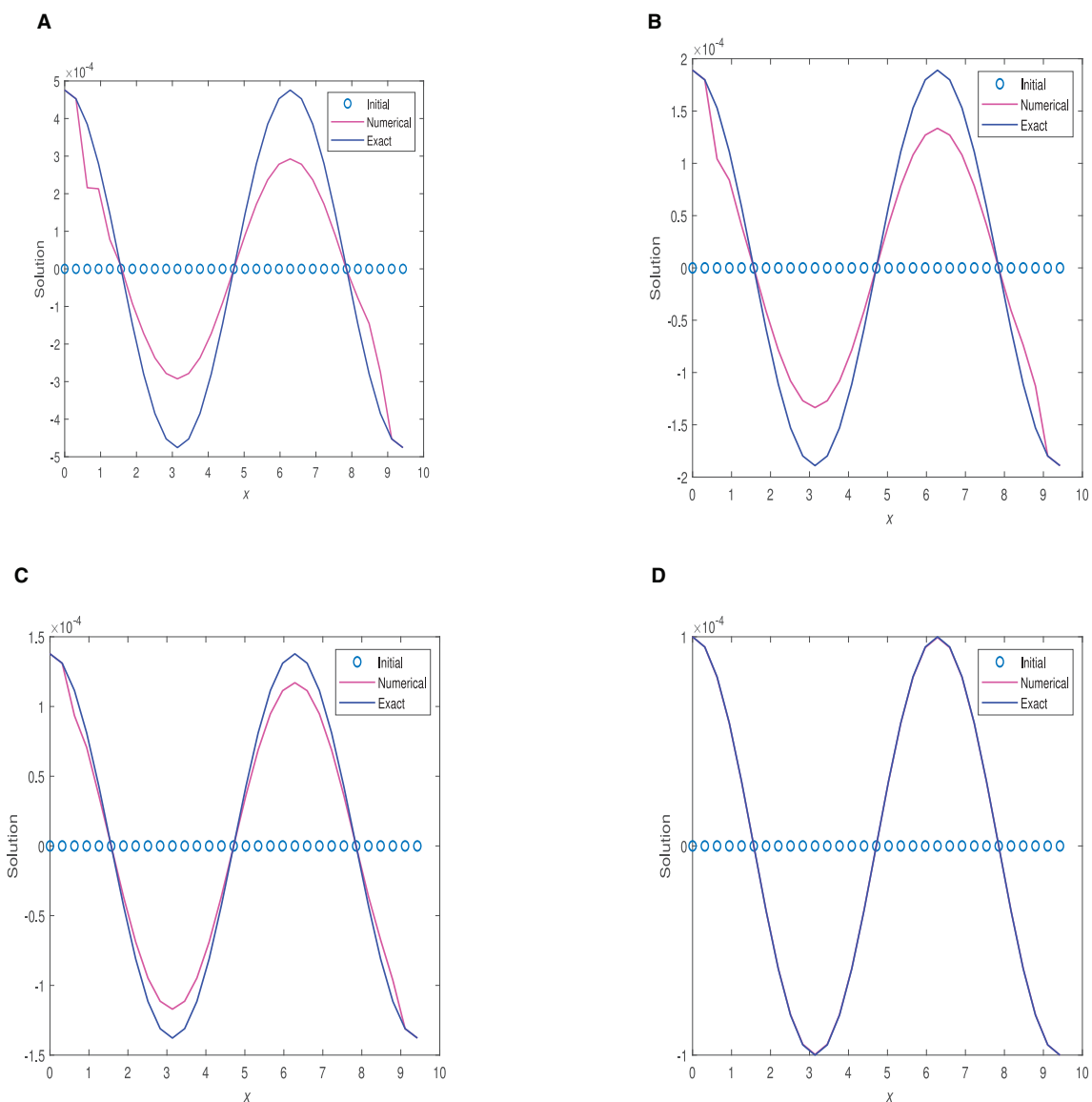


**FIGURE 8** Plots of exact solution and solution using FDMCA vs.  $x$  at time = 0.01 and different values of  $\alpha$ . (A)  $\alpha = 0.75$ ,  $\Delta t = 2.0 \times 10^{-3}$ . (B)  $\alpha = 0.90$ ,  $\Delta t = 2.0 \times 10^{-3}$ . (C)  $\alpha = 0.95$ ,  $\Delta t = 1.0 \times 10^{-3}$ . (D)  $\alpha = 1.0$ ,  $\Delta t = 3.125 \times 10^{-5}$ .

**TABLE 7** Range of values of  $\Delta t$  for stability of FDMCA scheme at some values of  $\alpha$ .

$\Delta x$	Values of $\alpha$	Range of values of $k$ for which $\xi_1 \leq 1.03$ .
$\frac{\pi}{10}$	$\alpha = 0.40$	$0 < k \leq 8.0 \times 10^{-6}$
	$\alpha = 0.75$	$0 < k \leq 8.0 \times 10^{-4}$
	$\alpha = 0.90$	$0 < k \leq 2.0 \times 10^{-3}$
	$\alpha = 0.95$	$0 < k \leq 2.0 \times 10^{-3}$

to approximately  $10^{-2}$  up to  $10^{-1}$ . The optimal step size appears to be  $2 \times 10^{-3}$  as indicated in Table 3.

At  $\alpha = 0.90$  and time 0.01, the FDMCO scheme produces very good results, with  $L_1$  errors of order  $10^{-5}$  and  $10^{-4}$ . The  $L_1$  errors are of order  $10^{-2}$  at time 0.1. The  $L_\infty$  error also exhibits some variation, ranging from  $10^{-5}$  to  $10^{-1}$  for all three time values  $t = 0.01, 0.1, 1.0$ .

At  $\alpha = 0.95$ , the scheme performs very well at time 0.01, and quite well at time 0.1. Quite satisfactorily results are obtained at time 0.1 when  $\Delta t = 4.0 \times 10^{-3}$ .

We have different behavior of FDMCO scheme at  $\alpha = 1.0$ . Good performance at all the times 0.01, 0.1, and 1.0. The general trend is as  $\Delta t$  decreases, the  $L_1$  error decreases at the three different values of time. The  $L_\infty$  error follows a similar trend, with errors ranging from approximately  $10^{-9}$  to  $10^{-3}$ .

TABLE 8  $L_1$  and  $L_\infty$  errors using  $\Delta x = \frac{\pi}{10}$  when  $\alpha = 0.40$  at different values of time.

Time	value of $\Delta t$	$L_1$ error	$L_\infty$ error
0.01	$3 \times 10^{-6}$	$3.964888 \times 10^{-3}$	$9.425055 \times 10^{-4}$
	$2 \times 10^{-6}$	$3.963746 \times 10^{-3}$	$9.422326 \times 10^{-4}$
	$1 \times 10^{-6}$	$3.962066 \times 10^{-3}$	$9.418269 \times 10^{-4}$
0.1	$5 \times 10^{-7}$	$3.918820 \times 10^{-1}$	$6.287411 \times 10^{-2}$
	$3.0 \times 10^{-6}$	3.983312	$6.392576 \times 10^{-1}$
	$2.0 \times 10^{-6}$	4.003418	$6.413542 \times 10^{-1}$
	$1.0 \times 10^{-6}$	4.052244	$6.613390 \times 10^{-1}$
	$5.0 \times 10^{-7}$	3.996515	$7.001752 \times 10^{-1}$

TABLE 9  $L_1$  and  $L_\infty$  errors using  $\Delta x = \frac{\pi}{10}$  when  $\alpha = 0.75$  at different values of time.

Time	value of $\Delta t$	$L_1$ error	$L_\infty$ error
0.01	$2 \times 10^{-3}$	$9.232497 \times 10^{-4}$	$1.831227 \times 10^{-4}$
	$1 \times 10^{-3}$	$6.860899 \times 10^{-4}$	$1.362180 \times 10^{-4}$
	$5 \times 10^{-4}$	$5.577237 \times 10^{-4}$	$1.107157 \times 10^{-4}$
	$2.5 \times 10^{-4}$	$4.894513 \times 10^{-4}$	$9.715393 \times 10^{-5}$
	$1.25 \times 10^{-4}$	$4.537029 \times 10^{-4}$	$9.005424 \times 10^{-5}$
	$6.25 \times 10^{-5}$	$4.351837 \times 10^{-4}$	$8.637680 \times 10^{-5}$
0.1	$3.125 \times 10^{-5}$	$4.256623 \times 10^{-4}$	$8.448622 \times 10^{-5}$
	$2 \times 10^{-3}$	$2.534690 \times 10^{-2}$	$5.866671 \times 10^{-3}$
	$1 \times 10^{-3}$	$2.380840 \times 10^{-2}$	$5.502920 \times 10^{-3}$
	$5 \times 10^{-4}$	$2.301513 \times 10^{-2}$	$5.314231 \times 10^{-3}$
1.0	$3.125 \times 10^{-5}$	$2.224258 \times 10^{-2}$	$5.130670 \times 10^{-3}$
	$5.0 \times 10^{-4}$	$1.076110 \times 10^0$	$3.047181 \times 10^{-1}$
	$2.5 \times 10^{-4}$	$1.073985 \times 10^0$	$3.041137 \times 10^{-1}$
	$1.25 \times 10^{-4}$	$1.072912 \times 10^0$	$3.038083 \times 10^{-1}$

TABLE 10  $L_1$  and  $L_\infty$  errors using  $\Delta x = \frac{\pi}{10}$  when  $\alpha = 0.90$  at different values of time

Time	value of $\Delta t$	$L_1$ error	$L_\infty$ error
0.01	$2 \times 10^{-3}$	$2.798512 \times 10^{-4}$	$5.553079 \times 10^{-5}$
	$1 \times 10^{-3}$	$1.841055 \times 10^{-4}$	$3.653084 \times 10^{-5}$
	$5 \times 10^{-4}$	$1.335701 \times 10^{-4}$	$2.650355 \times 10^{-5}$
0.1	$4 \times 10^{-3}$	$9.559487 \times 10^{-3}$	$2.100636 \times 10^{-3}$
	$2 \times 10^{-3}$	$7.905312 \times 10^{-3}$	$1.720222 \times 10^{-3}$
	$1 \times 10^{-3}$	$7.045737 \times 10^{-2}$	$1.524942 \times 10^{-3}$
	$5 \times 10^{-4}$	$6.601986 \times 10^{-3}$	$1.423985 \times 10^{-3}$
1.0	$2.0 \times 10^{-3}$	$4.220071 \times 10^{-1}$	$1.197178 \times 10^{-1}$
	$1.0 \times 10^{-3}$	$4.155238 \times 10^{-1}$	$1.178351 \times 10^{-1}$
	$5 \times 10^{-4}$	$4.122062 \times 10^{-1}$	$1.168730 \times 10^{-1}$

TABLE 11  $L_1$  and  $L_\infty$  errors using  $\Delta x = \frac{\pi}{10}$  when  $\alpha = 0.95$  at different values of time.

Time	value of time step $\Delta t$	$L_1$ error	$L_\infty$ error
0.01	$2 \times 10^{-3}$	$1.741426 \times 10^{-4}$	$3.455688 \times 10^{-5}$
	$1 \times 10^{-3}$	$1.043624 \times 10^{-4}$	$2.070903 \times 10^{-5}$
	$5 \times 10^{-4}$	$6.833858 \times 10^{-5}$	$1.356054 \times 10^{-5}$
	$6.25 \times 10^{-5}$	$3.540382 \times 10^{-5}$	$7.025210 \times 10^{-6}$
	$3.125 \times 10^{-5}$	$3.290969 \times 10^{-5}$	$6.530297 \times 10^{-6}$
0.1	$4 \times 10^{-3}$	$5.347467 \times 10^{-3}$	$1.166288 \times 10^{-3}$
	$2 \times 10^{-3}$	$4.042070 \times 10^{-3}$	$8.655839 \times 10^{-4}$
	$1 \times 10^{-3}$	$3.37315 \times 10^{-3}$	$7.140978 \times 10^{-4}$
	$5 \times 10^{-4}$	$3.030872 \times 10^{-3}$	$6.370183 \times 10^{-4}$
	$6.25 \times 10^{-5}$	$2.721195 \times 10^{-3}$	$5.674375 \times 10^{-4}$
	$3.125 \times 10^{-5}$	$2.698017 \times 10^{-3}$	$5.622326 \times 10^{-4}$
1.0	$4.0 \times 10^{-3}$	$3.904912 \times 10^0$	$1.155919 \times 10^0$
	$2.0 \times 10^{-3}$	$2.090670 \times 10^{-1}$	$5.946081 \times 10^{-2}$
	$1.0 \times 10^{-3}$	$2.036955 \times 10^{-1}$	$5.786996 \times 10^{-2}$
	$5.0 \times 10^{-4}$	$2.009656 \times 10^{-1}$	$5.705068 \times 10^{-2}$

TABLE 12  $L_1$  and  $L_\infty$  errors using  $\Delta x = \frac{\pi}{10}$  when  $\alpha = 1.0$  at different values of time.

Time	value of $\Delta t$	$L_1$ error	$L_\infty$ error
0.01	$2 \times 10^{-3}$	$1.007830 \times 10^{-4}$	$2.000000 \times 10^{-5}$
	$1 \times 10^{-3}$	$5.039313 \times 10^{-5}$	$1.000000 \times 10^{-5}$
	$5 \times 10^{-4}$	$2.519726 \times 10^{-5}$	$5.000002 \times 10^{-6}$
	$2.5 \times 10^{-4}$	$1.259910 \times 10^{-5}$	$2.500002 \times 10^{-6}$
	$1.25 \times 10^{-4}$	$6.299980 \times 10^{-6}$	$1.250001 \times 10^{-6}$
	$6.25 \times 10^{-5}$	$3.150940 \times 10^{-6}$	$6.250006 \times 10^{-7}$
	$3.125 \times 10^{-5}$	$1.576725 \times 10^{-6}$	$3.125003 \times 10^{-7}$
0.1	$2 \times 10^{-3}$	$9.958152 \times 10^{-4}$	$2.167634 \times 10^{-4}$
	$1 \times 10^{-3}$	$4.984131 \times 10^{-4}$	$1.088895 \times 10^{-4}$
	$2.5 \times 10^{-4}$	$1.262229 \times 10^{-4}$	$2.783164 \times 10^{-5}$
	$1.25 \times 10^{-4}$	$6.425759 \times 10^{-5}$	$1.431518 \times 10^{-5}$
	$6.25 \times 10^{-5}$	$3.486282 \times 10^{-5}$	$7.556457 \times 10^{-6}$
	$3.125 \times 10^{-5}$	$2.177843 \times 10^{-5}$	$4.541015 \times 10^{-6}$
1.0	$2.0 \times 10^{-3}$	$1.717096 \times 10^{-2}$	$3.878638 \times 10^{-3}$
	$1.0 \times 10^{-3}$	$1.558091 \times 10^{-2}$	$3.334386 \times 10^{-3}$
	$5.0 \times 10^{-4}$	$1.529808 \times 10^{-2}$	$3.165508 \times 10^{-3}$
	$2.5 \times 10^{-4}$	$1.522566 \times 10^{-2}$	$3.138913 \times 10^{-3}$
	$1.25 \times 10^{-4}$	$1.518925 \times 10^{-2}$	$3.126016 \times 10^{-3}$
	$6.25 \times 10^{-5}$	$1.517102 \times 10^{-2}$	$3.119640 \times 10^{-3}$
	$3.125 \times 10^{-5}$	$1.516189 \times 10^{-2}$	$3.116468 \times 10^{-3}$

In summary, the scheme’s performance relies on the value of the fractional parameter  $\alpha$  and the chosen time step  $\Delta t$ . Overall, the FDMCO scheme demonstrates considerable effectiveness for fractional parameter values that are close to 1.0.

As referred to in Section 2, we notice that

Based on Figures 5–7, we observe that:

- (i) FDMCO gives satisfactory performance at  $\alpha = 0.40$  and time 0.01 with maximum relative error being 14%.
- (ii) FDMCO is deemed satisfactory when  $\alpha = 0.95$ , time = 0.1 (with maximum relative error being 23.5%) and when  $\alpha = 0.90$ , time = 0.1 (with maximum relative error being about 23%).
- (iii) FDMCO is highly effective at  $\alpha = 1.0$  for the three times: 0.01, 0.1, and 1.0.

## 6 Finite difference method using Caputo derivative (FDMCA)

To numerically solve this equation, we employ an explicit finite difference scheme with Caputo’s approximation. The scheme to be constructed needs discretizing both spatial and time derivatives using central differences and incorporates the Caputo derivative with its L1 approximation [3].

Murio [35] derived an implicit scheme for a time-fractional diffusion equation. He approximated  $\frac{\partial^\alpha u}{\partial t^\alpha}$  as follows:

$$\begin{aligned} \frac{\partial^\alpha u(x_j, t_n)}{\partial t^\alpha} &= \frac{1}{\Gamma(1-\alpha)} \int_0^{t_n} \frac{\partial u(x_j, t)}{\partial t} \frac{1}{(t_n-t)^\alpha} dt \\ &= \frac{1}{\Gamma(1-\alpha)} \sum_{i=1}^n \int_{(i-1)k}^{ik} \left[ \frac{U_j^i - U_j^{i-1}}{k} + \Theta(k) \right] (nk-t)^{-\alpha} dt \\ &= \frac{1}{\Gamma(1-\alpha)} \sum_{i=1}^n \left\{ \left( \frac{U_j^i - U_j^{i-1}}{k} \right) \left[ \frac{(nk-t)^{-\alpha+1}}{-(1-\alpha)} \right]_{t=(i-1)k}^{t=ik} \right\} \\ &\quad + \frac{1}{\Gamma(1-\alpha)} \sum_{i=1}^n \left\{ \left[ \frac{(nk-t)^{-\alpha+1}}{-(1-\alpha)} \right]_{t=(i-1)k}^{t=ik} \right\} \cdot \Theta(k), \\ &= \frac{1}{\Gamma(1-\alpha)} \sum_{i=1}^n \left\{ \left( \frac{U_j^i - U_j^{i-1}}{k} \right) \left[ \frac{(nk-ik)^{-\alpha+1}}{-(1-\alpha)} \right] \right. \\ &\quad \left. + \frac{(nk-ik+k)^{-\alpha+1}}{(1-\alpha)} \right]_{t=(i-1)k}^{t=ik} \right\} \\ &\quad + \frac{1}{\Gamma(1-\alpha)} \sum_{i=1}^n \left\{ \left[ \frac{(nk-ik)^{-\alpha+1}}{-(1-\alpha)} \right] \right. \\ &\quad \left. + \frac{(nk-ik+k)^{-\alpha+1}}{(1-\alpha)} \right]_{t=(i-1)k}^{t=ik} \right\} \cdot \Theta(k), \\ &= \frac{1}{\Gamma(1-\alpha)} \sum_{i=1}^n \left\{ \left( \frac{U_j^i - U_j^{i-1}}{k} \right) \cdot k^{1-\alpha} \right. \\ &\quad \left. \cdot \left[ \frac{(n-i+1)^{1-\alpha} - (n-i)^{1-\alpha}}{-(1-\alpha)} \right]_{t=(i-1)k}^{t=ik} \right\} \end{aligned}$$

$$+ \frac{1}{\Gamma(1-\alpha)} \sum_{i=1}^n \left[ \frac{(n-i+1)^{1-\alpha} - (n-i)^{1-\alpha}}{-(1-\alpha)} \right]_{t=(i-1)k}^{t=ik} \cdot \Theta(k^{2-\alpha}).$$

For simplification, the formula  $\Gamma(2-\alpha) = (1-\alpha)\Gamma(1-\alpha)$  is used.

$$\begin{aligned} \frac{\partial^\alpha u(x_j, t_n)}{\partial t^\alpha} &\simeq \frac{k^{-\alpha}}{\Gamma(2-\alpha)} \sum_{i=1}^n \left\{ \left( U_j^i - U_j^{i-1} \right) \right. \\ &\quad \left. \cdot \left[ (n-i+1)^{1-\alpha} - (n-i)^{1-\alpha} \right] \right\}. \end{aligned}$$

This discretization gives rise to an implicit scheme. We attempt to discretize  $\frac{\partial^\alpha u(x_j, t_n)}{\partial t^\alpha}$  to construct an explicit scheme to solve the fractional KdV equation. We approximate  $\frac{\partial u(x,t)}{\partial t}$  by  $\frac{U_j^{i+1} - U_j^i}{k}$

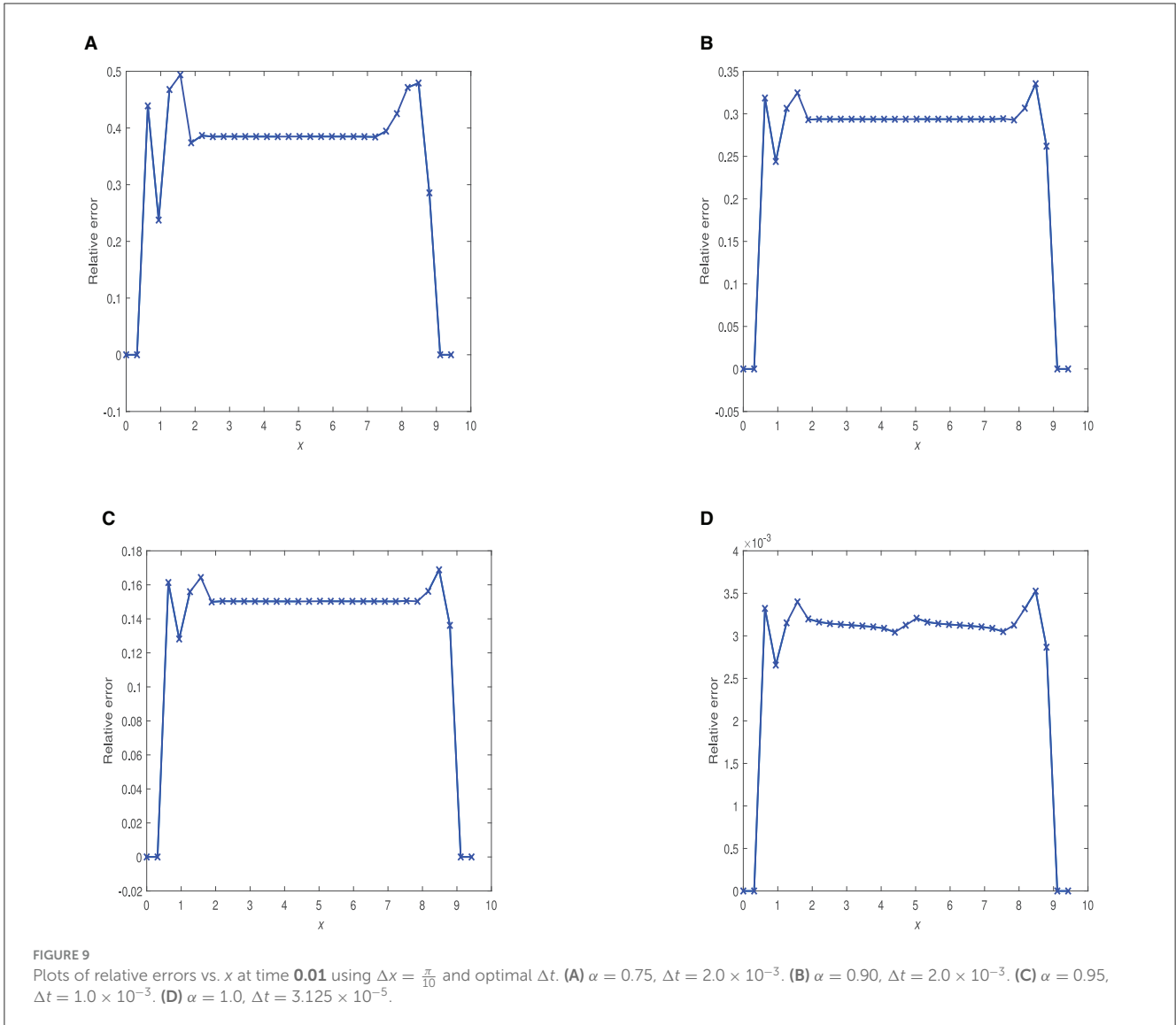
$$\begin{aligned} \frac{\partial^\alpha u(x_j, t_n)}{\partial t^\alpha} &= \frac{1}{\Gamma(1-\alpha)} \int_0^{t_n} \frac{\partial u(x_j, \tau)}{\partial \tau} (t_n-\tau)^{-\alpha} d\tau, \quad \text{where } t_n = nk, \\ &= \frac{1}{\Gamma(1-\alpha)} \sum_{i=1}^n \left\{ \int_{(i-1)k}^{ik} \left[ \frac{U_j^{i+1} - U_j^i}{k} + \Theta(k) \right] (nk-\tau)^{-\alpha} d\tau \right\} \\ &= \frac{1}{\Gamma(1-\alpha)} \sum_{i=1}^n \left\{ \left[ \frac{U_j^{i+1} - U_j^i}{k} + \Theta(k) \right] \int_{(i-1)k}^{ik} (nk-\tau)^{-\alpha} d\tau \right\} \\ &= \frac{1}{\Gamma(1-\alpha)} \sum_{i=1}^n \left\{ \left( \frac{U_j^{i+1} - U_j^i}{k} + \Theta(k) \right) \left[ \frac{-(nk-t)^{-\alpha+1}}{(1-\alpha)} \right]_{t=(i-1)k}^{t=ik} \right\} \\ &= \frac{k^{1-\alpha}}{(1-\alpha)\Gamma(1-\alpha)} \sum_{i=1}^n \left\{ \left( \frac{U_j^{i+1} - U_j^i}{k} + \Theta(k) \right) \right. \\ &\quad \left. \cdot \left[ (n-i+1)^{1-\alpha} - (n-i)^{1-\alpha} \right] \right\} \\ &= \frac{1}{(1-\alpha)\Gamma(1-\alpha)} \sum_{i=1}^n \left\{ \left( \frac{U_j^{i+1} - U_j^i}{k^\alpha} + \Theta(k^{2-\alpha}) \right) \right. \\ &\quad \left. \cdot \left[ (n-i+1)^{1-\alpha} - (n-i)^{1-\alpha} \right] \right\} \\ &\simeq \frac{1}{\Gamma(2-\alpha)} k^{-\alpha} \sum_{i=1}^n \left( U_j^{i+1} - U_j^i \right) \cdot \left[ (n-i+1)^{1-\alpha} - (n-i)^{1-\alpha} \right]. \end{aligned} \tag{20}$$

We note that

$$\begin{aligned} \sum_{i=1}^n \left( U_j^{i+1} - U_j^i \right) \cdot \left[ (n-i+1)^{1-\alpha} - (n-i)^{1-\alpha} \right] &= \left( U_j^2 - U_j^1 \right) (n^{1-\alpha} - (n-1)^{1-\alpha}) \\ &\quad + \left( U_j^3 - U_j^2 \right) ((n-1)^{1-\alpha} - (n-2)^{1-\alpha}) \\ &\quad + \left( U_j^4 - U_j^3 \right) ((n-2)^{1-\alpha} - (n-3)^{1-\alpha}) \\ &\quad + \left( U_j^5 - U_j^4 \right) ((n-3)^{1-\alpha} - (n-4)^{1-\alpha}) \\ &\quad + \dots + \left( U_j^n - U_j^{n-1} \right) (2^{1-\alpha} - 1^{1-\alpha}) \\ &\quad + \left( U_j^{n+1} - U_j^n \right) (1^{1-\alpha} - 0), \end{aligned}$$

which can be written as

$$U_j^{n+1} - U_j^n + \sum_{i=1}^{n-1} \left[ (i+1)^{1-\alpha} - i^{1-\alpha} \right] \left( U_j^{n-i+1} - U_j^{n-i} \right).$$



Hence,

$$\frac{\partial^\alpha u(x_j, t_n)}{\partial t^\alpha} \simeq \frac{1}{\Gamma(2-\alpha)} \frac{1}{k^\alpha} \left\{ U_j^{n+1} - U_j^n + \sum_{i=1}^{n-1} \left( U_j^{n-i+1} - U_j^{n-i} \right) \left[ (i+1)^{1-\alpha} - i^{1-\alpha} \right] \right\}. \quad (21)$$

$$+ \frac{U_{j+1}^n - U_{j-1}^n}{2 \cdot (\Delta x)} + \frac{U_{j+2}^n - 2U_{j+1}^n + 2U_{j-1}^n - 2U_{j-2}^n}{2 \cdot (\Delta x)^3} = 2t_n \cos(x_j). \quad (23)$$

We therefore have

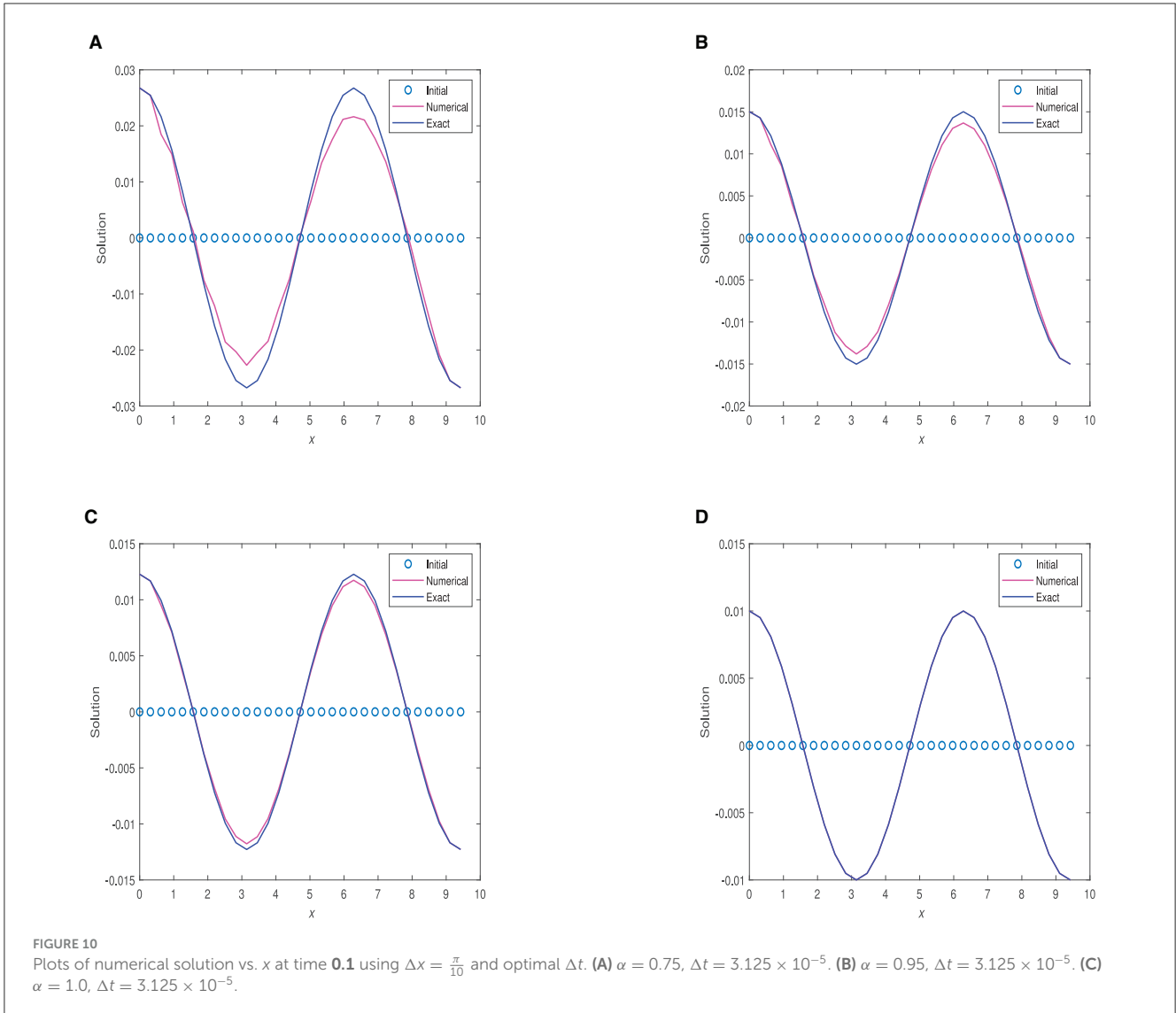
### 6.1 Derivation of FDMCA scheme

FDMCA when used to discrete Equation (1) is given by

$$\frac{k^{-\alpha}}{\Gamma(2-\alpha)} \left( U_j^{n+1} - U_j^n \right) + \frac{k^{-\alpha}}{\Gamma(2-\alpha)} \sum_{i=1}^{n-1} \left( U_j^{n-i+1} - U_j^{n-i} \right) \left[ (i+1)^{1-\alpha} - i^{1-\alpha} \right] \quad (22)$$

$$U_j^{n+1} = U_j^n - \frac{k^{-\alpha}}{\Gamma(2-\alpha)} \sum_{i=1}^{n-1} \left( U_j^{n-i+1} - U_j^{n-i} \right) \left[ (i+1)^{1-\alpha} - i^{1-\alpha} \right] - \frac{U_{j+1}^n - U_{j-1}^n}{2 \cdot (\Delta x)} \cdot k^\alpha \cdot \Gamma(2-\alpha) - \frac{\Gamma(2-\alpha) \cdot k^\alpha}{2 \cdot (\Delta x)^3} \left( U_{j+2}^n - 2U_{j+1}^n + 2U_{j-1}^n - 2U_{j-2}^n \right) \quad (24)$$

$$+ k^\alpha \cdot \Gamma(2-\alpha) 2t_n \cos(x_j). \quad (25)$$



### 6.2 Stability of FDMCA scheme

To study the stability of FDMCA scheme, we consider the following equation

$$\begin{aligned}
 U_j^{n+1} &= U_j^n - \sum_{i=1}^{n-1} (U_j^{n+1-i} - U_j^{n-i}) ((i+1)^{1-\alpha} - i^{1-\alpha}) \\
 &\quad - \left( \frac{U_{j+1}^n - U_{j-1}^n}{2 \cdot (\Delta x)} \right) \cdot k^\alpha \cdot \Gamma(2-\alpha) \\
 &\quad - \frac{\Gamma(2-\alpha) \cdot k^\alpha}{2 \cdot (\Delta x)^3} (U_{j+2}^n - 2U_{j+1}^n + 2U_{j-1}^n - 2U_{j-2}^n).
 \end{aligned}
 \tag{26}$$

We then substitute  $U_j^n$  by  $\xi^n e^{j\omega}$  where  $\omega = \theta h$ , where  $\theta$  is the wave number and  $I = \sqrt{-1}$ . This gives

$$\xi^{n+1} e^{j\omega} = \xi^n e^{j\omega} - \sum_{i=1}^{n-1} \xi^{n+1-i} (e^{j\omega} - \xi^{n-i} e^{j\omega}) \cdot ((i+1)^{1-\alpha} - i^{1-\alpha})$$

$$\begin{aligned}
 & - \xi^n e^{j\omega} \left( \frac{e^{I\omega} - e^{-I\omega}}{2 \cdot (\Delta x)} \right) \cdot \Gamma(2-\alpha) \cdot k^\alpha \\
 & - \frac{\xi^n \cdot \Gamma(2-\alpha) \cdot k^\alpha}{2 \cdot (\Delta x)^3} \cdot e^{j\omega} \cdot (e^{2I\omega} - 2e^{I\omega} + 2e^{-I\omega} - e^{-2I\omega}).
 \end{aligned}$$

Upon simplification, we get

$$\begin{aligned}
 \xi^{n+1} &= \xi^n \left\{ 1 - \frac{2I \sin(\omega)}{2h} \cdot \Gamma(2-\alpha) \cdot k^\alpha \right. \\
 &\quad - \frac{\Gamma(2-\alpha)}{2h^3} \cdot (2I \sin(2\omega) - 4I \sin(\omega)) \\
 &\quad \left. - \sum_{i=1}^{n-1} (\xi^{n+1-i} - \xi^{n-i}) ((i+1)^{1-\alpha} - i^{1-\alpha}) \right\}.
 \end{aligned}
 \tag{27}$$

$$\tag{28}$$

(i) We take the case  $n = 1$ :

$$|\xi| = \left\{ 1 + \left[ \frac{\sin(\omega)}{h} \Gamma(2-\alpha) \cdot k^\alpha + \frac{\Gamma(2-\alpha)}{2h^3} \cdot k^\alpha \right] \right\}
 \tag{29}$$



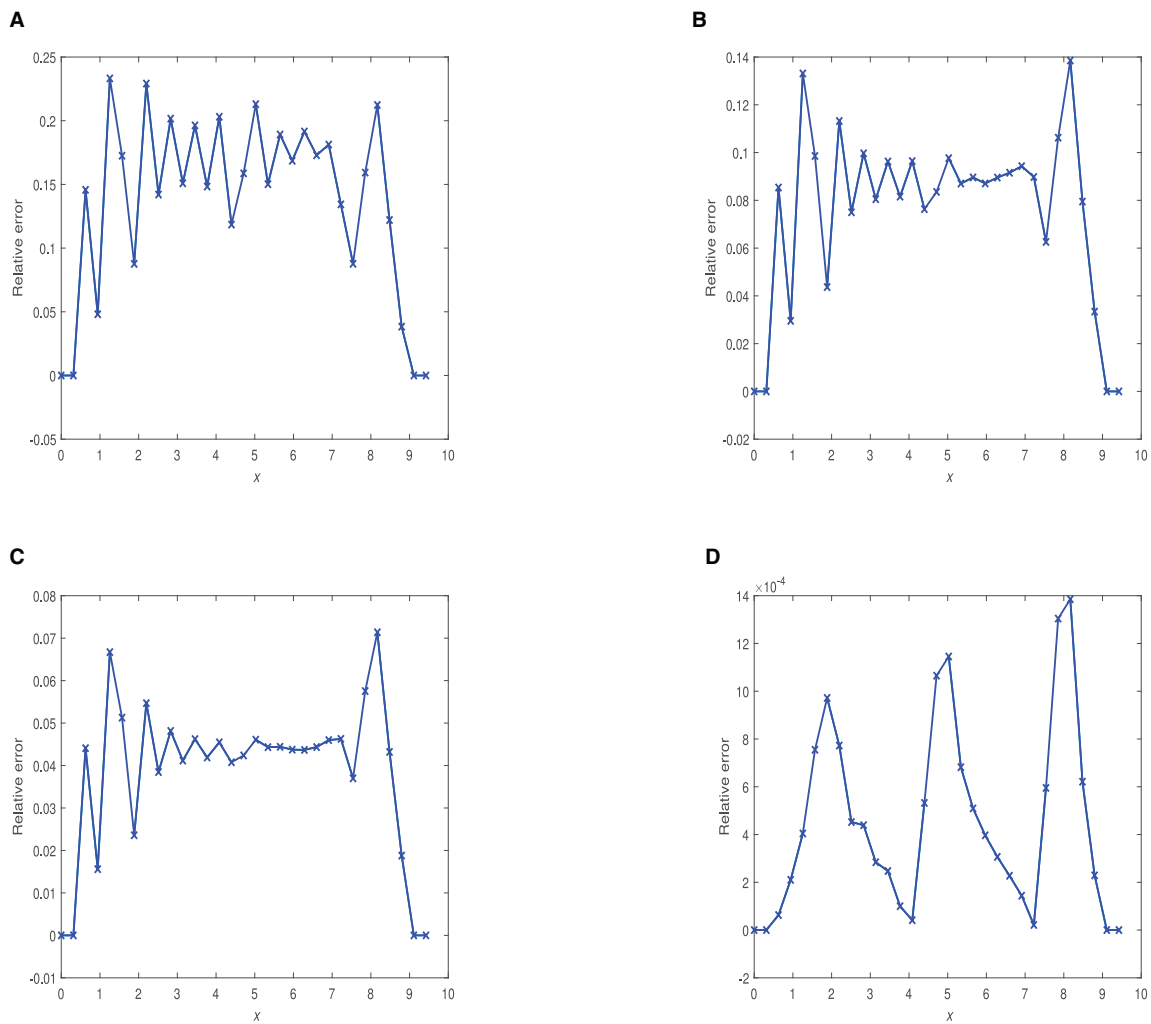


**FIGURE 11** Plots of relative errors vs.  $x$  at time  $0.1$  using  $\Delta x = \frac{\pi}{10}$  and optimal  $\Delta t$ . **(A)**  $\alpha = 0.75$ ,  $\Delta t = 3.125 \times 10^{-5}$ . **(B)**  $\alpha = 0.90$ ,  $\Delta t = 5.0 \times 10^{-4}$ . **(C)**  $\alpha = 0.95$ ,  $\Delta t = 3.125 \times 10^{-5}$ . **(D)**  $\alpha = 1.0$ ,  $\Delta t = 3.125 \times 10^{-5}$ .

$$\cdot (2 \sin(2\omega) - 4 \sin(\omega)) \Big]^{1/2}. \quad (30)$$

The scheme is unstable when  $n = 1$ .

(ii) For the case  $n = 2$ , we get a quadratic equation in  $\xi$ :

$$\xi^2 + \xi (2^{1-\alpha} - B - 1) - (2^{1-\alpha} - 1) = 0,$$

where

$$B = 1 - \frac{I \sin(\omega)}{h} \cdot \Gamma(2 - \alpha) \cdot k^\alpha - \frac{\Gamma(2 - \alpha)}{2h^3} \quad (31)$$

$$\cdot k^\alpha \cdot (2I \sin(2\omega) - 4I \sin(\omega)). \quad (32)$$

This gives

$$\xi_{1,2} = \frac{B + 1 - 2^{1-\alpha} \pm \sqrt{(2^{1-\alpha} - B - 1)^2 + 4(2^{1-\alpha} - 1)}}{2}. \quad (33)$$

We plot  $|\xi_1|$  vs.  $\omega \in [-\pi, \pi]$  vs.  $k$  and  $|\xi_2|$  vs.  $\omega \in [-\pi, \pi]$  vs.  $k$  for the five cases:  $\alpha = 0.40, 0.75, 0.90, 0.95, 1.0$ .

It is seen that  $|\xi_2| < 1$  for all values of  $k > 0$  and  $\omega \in [-\pi, \pi]$ . However,  $|\xi_1| \geq 1$  for  $k > 0$  and  $\omega \in [-\pi, \pi]$ .

We obtain some range of values of  $k$  for which scheme is mildly stable, in that case, we choose  $|\xi_1| \leq 1.03$  and the results are showed in [Table 7](#).

We see that as we increase  $n$  and keep  $\alpha$  fixed, the stability limit for  $k$  increases. If we keep  $\alpha$  fixed and increase  $n$ , the stability region for  $k$  is enlarged.

As  $n$  get larger, the expression for the amplification factor gets more complicated and stability analysis become difficult for the explicit FDMCA scheme. We plan in future to construct NSFDM methods using Caputo approximations or construct implicit versions of FDMCA scheme.

**Remark 1.** We would like to point out that for the case when  $\alpha = 1.0$ , the stability is straightforwardly established, similar to the classical KdV approach demonstrated in our previous studies in Appadu and Kelil [10] and Kelil [36].

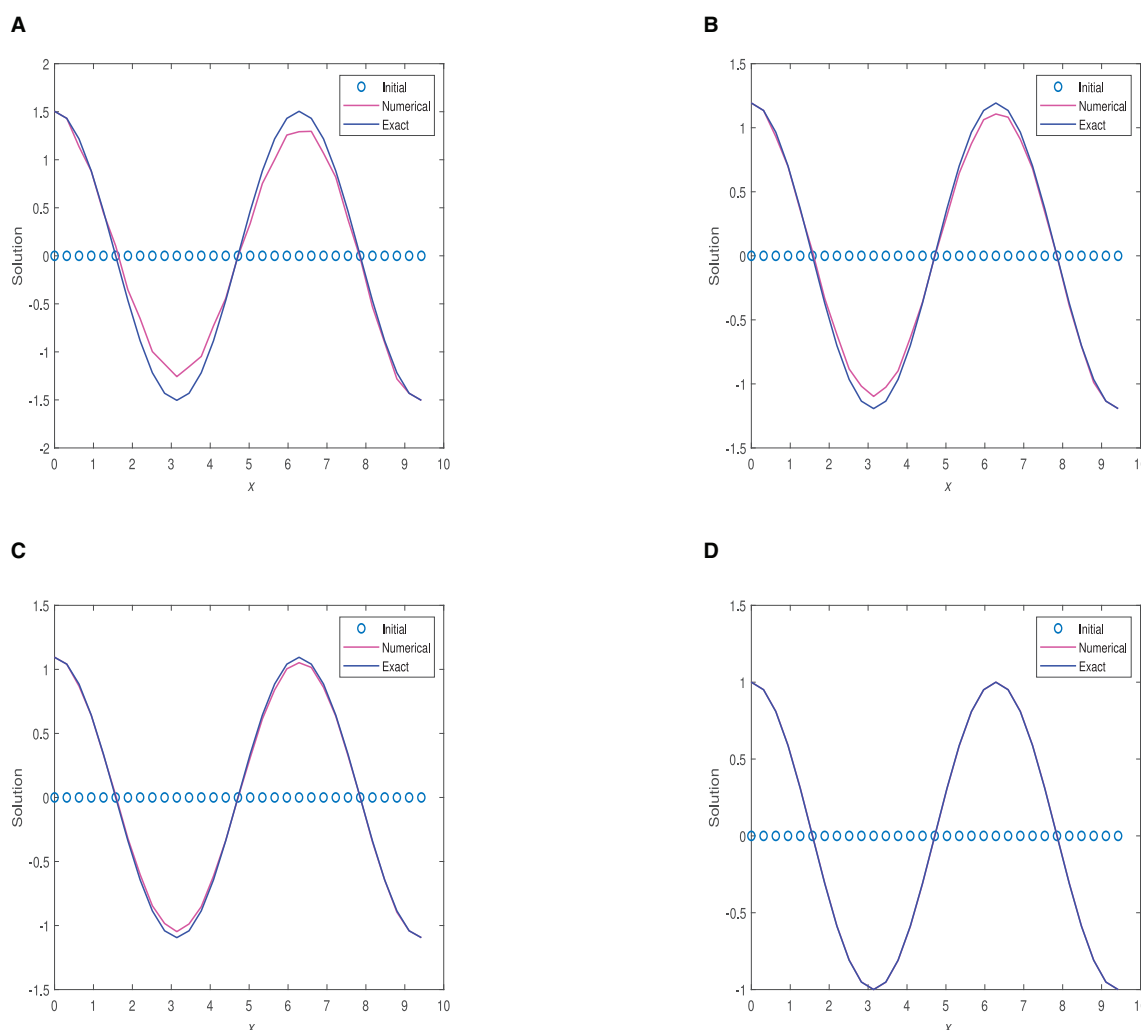


**FIGURE 12** 2D plots of numerical solution vs.  $x$  at time **1.0** using  $\Delta x = \frac{\pi}{10}$  and optimal  $\Delta t$ . **(A)**  $\alpha = 0.75$ ,  $\Delta t = 1.25 \times 10^{-4}$ . **(B)**  $\alpha = 0.90$ ,  $\Delta t = 5.0 \times 10^{-4}$ . **(C)**  $\alpha = 0.95$ ,  $\Delta t = 5.0 \times 10^{-4}$ . **(D)**  $\alpha = 1.0$ ,  $\Delta t = 3.125 \times 10^{-5}$ .

## 7 Numerical results: FDMCA scheme

In this section, we present some numerical profiles for the FDMCA scheme to solve the non-homogeneous KdV equation. We now compute the accuracy of the numerical solution and also the performance of the scheme by computing  $L_1$  and  $L_\infty$  errors. We compare the numerical solutions obtained by both schemes for Equation (1) with its exact solution. Numerical calculations are carried out by using Matlab and Maple 18 on an Intel@Core i5 2.30GHz with 8 GB RAM and 64-bit operating system (Windows 10).

### 7.1 Display of $L_1$ & $L_\infty$ errors (FDMCA)

We present in Tables 8–12, the  $L_1$  and  $L_\infty$  errors at different times and various  $\Delta t$  values for five specific cases:  $\alpha$  values of 0.40, 0.75, 0.90, 0.95, and 1.0. It is noteworthy that for all our

experiments, we chose  $\Delta x = \frac{\pi}{10}$  and appropriately chosen  $\Delta t$  to ensure feasible solution profiles, as revealed in Figures 8–12 for three values of time  $t = 0.01, 0.1, 1.0$ .

FDMCA is much better than FDMCO at  $\alpha = 0.40$  for time 0.01. Moreover, FDMCA gives better results than FDMCO at  $\alpha = 0.75, 0.90, 0.95$  for all the three times 0.01, 0.1, 1.0.

### 7.2 Numerical profiles and relative errors: FDMCA

In this section, we present graphical comparisons of numerical solutions for  $x$  for five different  $\alpha$ -values at three specific time points: 0.01, 0.1, and 1.0. These plots were generated using an appropriately selected  $\Delta t$  and a fixed grid spacing of  $\Delta x = \frac{\pi}{10}$ .

Figure 8 displays 2D plots of the numerical solution at  $t = 0.01$ . Figure 10 shows numerical solution graphs at  $t = 0.1$ . Figure 12

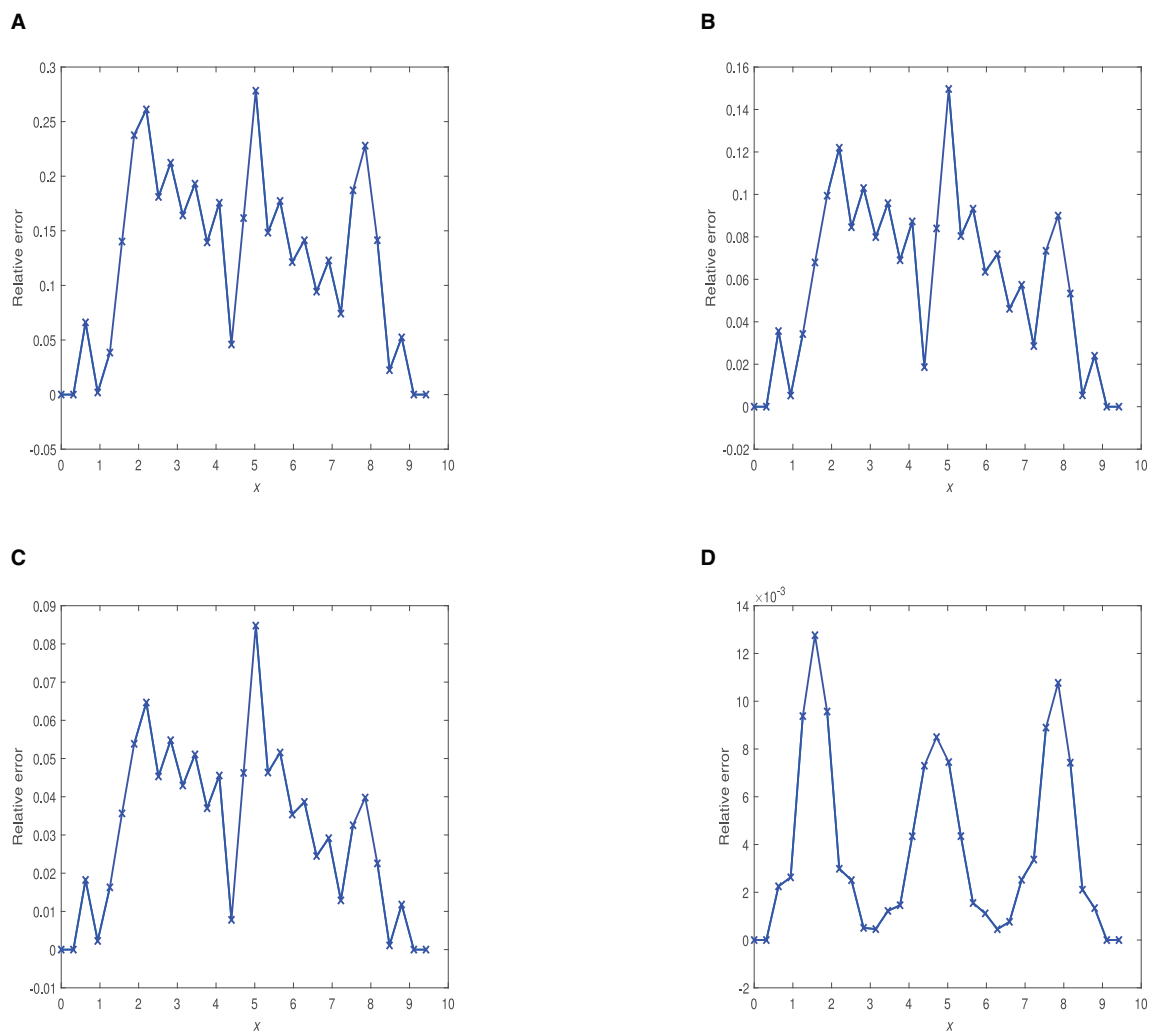


**FIGURE 13**  
 Plots of relative errors vs.  $x$  at time **1.0** using  $\Delta x = \frac{\pi}{10}$  and for some appropriately chosen optimal  $\Delta t$ . **(A)**  $\alpha = 0.75$ ,  $\Delta t = 1.25 \times 10^{-4}$ . **(B)**  $\alpha = 0.90$ ,  $\Delta t = 5.0 \times 10^{-4}$ . **(C)**  $\alpha = 0.95$ ,  $\Delta t = 5.0 \times 10^{-4}$ . **(D)**  $\alpha = 1.0$ ,  $\Delta t = 3.125 \times 10^{-5}$ .

demonstrates numerical solution plots at  $t = 1.0$ , utilizing  $\alpha$ -values of 0.40, 0.75, 0.90, 0.95, and 1.0. Additionally, Figures 9, 11, 13 present graphs depicting the relative errors with respect to  $x$  for the FDMCA scheme at these three specific time points.

At time 0.01, FDMCA is not effective at  $\alpha = 0.75$  and  $\alpha = 0.90$ . However, the scheme gives satisfactory performance with maximum relative error being 18%. The scheme displays excellent performance when  $\alpha = 1.0$  with maximum relative error of  $4.0 \times 10^{-1}\%$ .

FDMCA is highly effective at  $\alpha = 0.95$ ,  $\alpha = 1.0$  when time is 0.1 with maximum relative error being 8% and  $14 \times 10^{-2}\%$ , respectively. The scheme is deemed satisfactory at  $\alpha = 0.75$ ,  $\alpha = 0.90$  when time of propagation is 0.1.

FDMCA is highly effective at  $\alpha = 0.95$ ,  $\alpha = 1.0$  when time is 1.0 with maximum relative error being 8.5% and  $13 \times 10^{-1}\%$ , respectively. The scheme is deemed satisfactory at  $\alpha = 0.75$ ,  $\alpha = 0.90$  when time of propagation is 1.0.

## 8 Conclusion

In this study, we have constructed two finite difference schemes to solve a non-homogeneous fractional dispersive Korteweg-de Vries (KdV) equation. We utilized both conformable and Caputo derivatives in our numerical methods and conducted a comprehensive analysis of their qualitative properties, including stability, consistency, and error analysis using both  $L_1$  and  $L_\infty$  error norms. We presented tables and plots showing relative errors and provided graphical representations of numerical profiles for both schemes. When working with the FDMCO scheme, we observed the following scenarios at five different fractional parameter values  $\alpha = 0.40, 0.75, 0.90, 0.95, 1.0$  and at different times, including those as follows:

- At  $\alpha = 0.75, 0.90, 0.95, 1.0$  at time  $t = 0.01$ .
- At  $\alpha = 0.90, 0.95, 1.0$  at time  $t = 0.1$ .
- At  $\alpha = 0.90, 0.95, 1.0$  at time  $t = 1.0$ .

The FDMCA scheme yielded particularly good results for fractional values of  $\alpha$  ranging from 0.75 up to 1.0, as evidenced by the tabulated data and accompanying figures. In general, the performance of both schemes is closely related to the fractional parameter  $\alpha$  and the chosen time step  $\Delta t$ . We notice that both FDMCO and FDMCA schemes exhibit significant effectiveness, particularly when dealing with fractional parameter values that approach 1.0. When comparing the fractional parameter range  $\alpha \in (0.40, 1.0]$ , the FDMCA scheme outperforms the FDMCO scheme.

## Data availability statement

The raw data supporting the conclusions of this article will be made available by the authors, without undue reservation.

## Author contributions

AA: Conceptualization, Formal analysis, Investigation, Methodology, Project administration, Resources, Software, Supervision, Validation, Visualization, Writing – original draft, Writing – review & editing. AK: Formal analysis, Funding acquisition, Investigation, Methodology, Resources, Software, Validation, Visualization, Writing – original draft.

## References

- Podlubny I. *Fractional Differential Equations, Mathematics in Science and Engineering*. New York: Academic press. (1999).
- Miller KS, Ross B. *An Introduction to the Fractional Calculus and Fractional Differential Equations*. New York: John Wiley and Sons. (1993).
- Oldham K, Spanier J. *The Fractional Calculus Theory and Applications of Differentiation and Integration to Arbitrary Order*. London: Elsevier. (1974).
- Podlubny I. *Fractional Differential Equations: An Introduction to Fractional Derivatives, Fractional Differential Equations, to Methods of Their Solution and Some of Their Applications*. London: Elsevier. (1998).
- Eriqat T, Oqielat MN, Al-Zhour Z, Khammash GS, El-Ajou A, Alrabaiah H. Exact and numerical solutions of higher-order fractional partial differential equations: a new analytical method and some applications. *Pramana*. (2022) 96:207. doi: 10.1007/s12043-022-02446-4
- Kordeweg D, de Vries G. On the change of form of long waves advancing in a rectangular channel, and a new type of long stationary wave. *Philos Mag*. (1895) 39:422–43. doi: 10.1080/14786449508620739
- Appadu AR, Kelil AS. On semi-analytical solutions for linearized dispersive KdV equations. *Mathematics*. (2020) 8:1769. doi: 10.3390/math8101769
- He JH. Homotopy perturbation technique. *Comput Methods Appl Mech Eng*. (1999) 178:257–62. doi: 10.1016/S0045-7825(99)0018-3
- Kelil AS, Appadu AR. On the numerical solution of 1D and 2D KdV equations using variational homotopy perturbation and finite difference methods. *Mathematics*. (2022) 10:4443. doi: 10.3390/math10234443
- Appadu AR, Kelil AS. Comparison of modified ADM and classical finite difference method for some third-order and fifth-order KdV equations. *Demonstr Mathem*. (2021) 54:377–409. doi: 10.1515/dema-2021-0039
- Sewell G. *Analysis of a Finite Element Method: PDE/PROTRAN*. Cham: Springer Science & Business Media. (2012).
- Aderogba AA, Appadu AR. Classical and multisymplectic schemes for linearized KdV equation: numerical results and dispersion analysis. *Fluids*. (2021) 6:214. doi: 10.3390/fluids6060214
- Rostamy D, Alipour M, Jafari H, Baleanu D. Solving multi-term orders fractional differential equations by operational matrices of BPs with convergence analysis. *Rom Rep Phys*. (2013) 65:334–49.
- Anwar A, Jarad F, Baleanu D, Ayaz F. Fractional Caputo heat equation within the double Laplace transform. *Rom J Phys*. (2013) 58:15–22.
- Jumarie G. Table of some basic fractional calculus formulae derived from a modified Riemann-Liouville derivative for non-differentiable functions. *Appl Math Lett*. (2009) 22:378–85. doi: 10.1016/j.aml.2008.06.003
- Khalil R, Al Horani M, Yousef A, Sababheh M. A new definition of fractional derivative. *J Comput Appl Math*. (2014) 264:65–70. doi: 10.1016/j.cam.2014.01.002
- Toptakseven S. Numerical solutions of conformable fractional differential equations by Taylor and finite difference methods. *Sileyman Demirel Üniversitesi Fen Bilimleri Enstitüsü Dergisi*. (2019) 23:850–863. doi: 10.19113/sdufenbed.579361
- Li X, Xu C, A. space-time spectral method for the time fractional diffusion equation. *SIAM J Numer Anal*. (2009) 47:2108–31. doi: 10.1137/080718942
- Lin Y, Xu C. Finite difference/spectral approximations for the time-fractional diffusion equation. *J Comput Phys*. (2007) 225:1533–52. doi: 10.1016/j.jcp.2007.02.001
- Mohyud-Din ST, Yıldırım A, Yüklükü E. Homotopy analysis method for space- and time-fractional KdV equation. *Int J Numer Methods Heat Fluid Flow*. (2012) 22:928–41. doi: 10.1108/09615531211255798
- Abdeljawad T. On conformable fractional calculus. *J Comput Appl Math*. (2015) 279:57–66. doi: 10.1016/j.cam.2014.10.016
- Diethelm K, Ford NJ. Analysis of fractional differential equations. *J Math Anal Appl*. (2002) 265:229–48. doi: 10.1006/jmaa.2000.7194
- Kilbas AA, Srivastava HM, Trujillo JJ. *Theory and Applications of Fractional Differential Equations*. New York, NY: Elsevier. (2006).
- Caputo M. Linear models of dissipation whose Q is almost frequency independent. *Geophy J Int*. (1967) 13:529–39. doi: 10.1111/j.1365-246X.1967.tb02303.x
- Baleanu D, Diethelm K, Scalas E, Trujillo JJ. *Fractional Calculus: Models and Numerical Methods*. New York, NY: World Scientific. (2012). doi: 10.1142/8180
- Nakagawa J, Sakamoto K, Yamamoto M. Overview to mathematical analysis for fractional diffusion equations: new mathematical aspects motivated by industrial collaboration. *J Math Ind*. (2010) 2:99–108.
- Yokus A, Durur H, Kaya D, Ahmad H, Nofal TA. Numerical comparison of Caputo and Conformable derivatives of time fractional Burgers-Fisher equation. *Results Phys*. (2021) 25:104247. doi: 10.1016/j.rinp.2021.104247

## Funding

The author(s) declare financial support was received for the research, authorship, and/or publication of this article. AA is grateful to Nelson Mandela University, where the work was carried out. AK is grateful for postdoctoral research funding from NRF scarce skills fellowship under grant No. 138521.

## Conflict of interest

The authors declare that the research was conducted in the absence of any commercial or financial relationships that could be construed as a potential conflict of interest.

## Publisher's note

All claims expressed in this article are solely those of the authors and do not necessarily represent those of their affiliated organizations, or those of the publisher, the editors and the reviewers. Any product that may be evaluated in this article, or claim that may be made by its manufacturer, is not guaranteed or endorsed by the publisher.

28. Atangana A, Baleanu D, Alsaedi A. Analysis of time-fractional Hunter-Saxton equation: a model of nematic liquid crystal. *Open Phys.* (2016) 14:145–9. doi: 10.1515/phys-2016-0010
29. Atangana A, Secer A. The time-fractional coupled-Korteweg-de-Vries equations. In: *Abstract and Applied Analysis* (Hindawi) (2013). doi: 10.1155/2013/947986
30. Yokus A, Yavuz M. Novel comparison of numerical and analytical methods for fractional Burger-Fisher equation. *Discr Contin Dynam Syst S.* (2021) 14:2591–2606. doi: 10.3934/dcdss.2020258
31. Pedram L, Rostamy D. Numerical simulations of stochastic conformable space-time fractional Korteweg-de Vries and Benjamin-Bona-Mahony equations. *Nonl Eng.* (2021) 10:77–90. doi: 10.1515/nleng-2021-0007
32. Arafa AA, Rashed Z, Ahmed SE. Radiative flow of non Newtonian nanofluids within inclined porous enclosures with time fractional derivative. *Sci Rep.* (2021) 11:5338. doi: 10.1038/s41598-021-84848-9
33. Mous I, Laouar A. A numerical solution of a coupling system of conformable time-derivative two-dimensional Burger's equations. *Kragujevac J Mathem.* (2024) 48:7–23.
34. Azerad P, Bouharguane A. Finite difference approximations for a fractional diffusion/anti-diffusion equation. *arXiv preprint arXiv:11044861.* (2011).
35. Murio DA. Implicit finite difference approximation for time fractional diffusion equations. *Comput Mathem Appl.* (2008) 56:1138–45. doi: 10.1016/j.camwa.2008.02.015
36. Kelil AS. Comparative study of some numerical and semi-analytical methods for some 1D and 2D dispersive KdV-type equations. *Fundam Contem Mathem Sci.* (2022) 3:1–25. doi: 10.54974/fcmathsci.1002281